Zeitschrift: IABSE reports = Rapports AIPC = IVBH Berichte
Band: 75 (1996)

Rubrik: Session 8: Design of frames

SESSION 8

DESIGN OF FRAMES

Leere Seite
Blank page
Page vide

A NEW DESIGN APPROACH FOR BRACED FRAMES WITH EXTENDED END PLATE CONNECTIONS

Ciro Faella
Department of Civil Engineering, University of Salerno, Italy

Ciro Faella, born 1947, received his Civil Engineering degree in 1971 at the University of Naples (Italy). National Technical Contact (NTC) for CEN/TC250/SC3 dealing with construction and design of steel bridges, presently he is Full Professor of Structural Engineering at the Department of Civil Engineering of Salerno University. He is carrying out research on reinforced concrete, steel and composite structures.

Vincenzo Piluso
Department of Civil Engineering, University of Salerno, Italy

Vincenzo Piluso, born 1962, graduated in Civil Engineering in 1987 from the Naples University (Italy) where also received his PhD degree in Structural Engineering in 1992. Full member and secretary of ECCS TC13 on Seismic Design and member of COST C1, presently he is researcher at the Department of Civil Engineering of Salerno University. His activity is mainly devoted to steel structures and seismic engineering.

Gianvittorio Rizzano
Department of Civil Engineering, University of Salerno, Italy

Gianvittorio Rizzano, born 1962, graduated in Civil Engineering from the Naples University (Italy) in 1987, received is PhD degree in Structural Engineering in 1995. Presently he is research assistant at the Department of Civil Engineering of Salerno University. His field of research mainly concerns steel and reinforced concrete structures.

Summary

The main difficulty to be faced in designing semirigid frames is that the design internal actions of joints depend on the joint rotational behaviour which, in turn, can be determined provided that the joints have been completely detailed. As a consequence, any design method requires many iterations to achieve safe solutions. With reference to braced frames, a new design procedure able to overcome this difficulty is presented in this paper.

The proposed design approach is based on the use of design abaci, developed by the same authors in previous works, relating the joint rotational behaviour to the main geometrical parameters of the structural detail. The innovative feature of the proposed design procedure is its ability to guide the designer up to the complete detailing of beam-to-column connections. Finally, a design example is presented to show the practical application of the proposed design procedure.

1. Introduction

Even though the semirigidity concept has been introduced many years ago, steel structures are usually designed by assuming that beam-to-column joints are either pinned or rigid. This design assumption allows a great simplification in structural analysis, but it neglects the true behaviour of joints.

The economic and structural benefits of semirigid connections are well known and much has been written about their use in braced frames. The main advantages they provide over pinned frames are the reduction of the mid-span moments and of the column effective length. Notwithstanding, they are seldom used by designers, because most semirigid connections have highly nonlinear behaviour so that the analysis and design of frames using them is difficult. In particular, the design problem becomes more difficult as soon as the true rotational behaviour of beam-to-column joints is accounted for, because the internal actions that members and joints have to withstand, depend on the joint rotational stiffness. As the joint flexural resistance is strictly related to its rotational stiffness, the design problem requires some attempts to achieve a safe and economical design.

In the case of braced frames, the beam line method is commonly used to face the design problem, but it does not provide any indication regarding the detailing of beam-to-column joints. In other words, as it is difficult to design joints having predetermined values of rotational stiffness and flexural resistance, the most important point in designing semirigid frames is practically still to be solved. For this reason, within a strategic programme

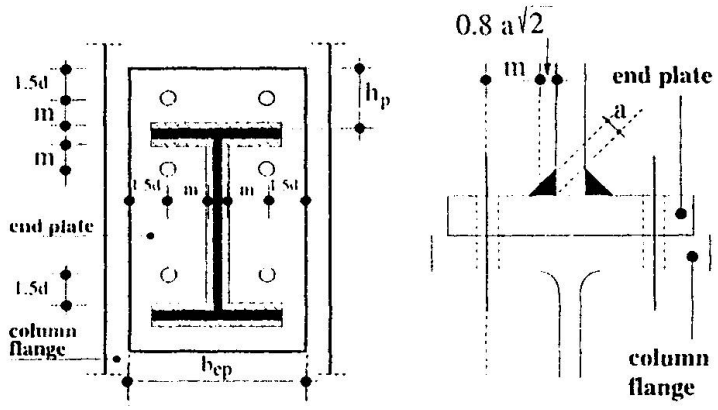

Fig.1 - Geometrical detail of the analysed joints

«SPRINT» of the European Community [1], tables giving the rotational stiffness and the flexural strength of a great number of joints for different connection typologies have been prepared to provide designers with an important help in designing semirigid frames, allowing the exploitation of the benefits of this structural typology.

Despite the great number of considered cases, these tables do not represent an exhaustive solution of the design problem. For this reason, with reference to extended end plate connections a new design procedure is herein proposed with the aim to guide the designer up to the complete detailing of beam-to-column joints.

2. Design of extended end plate connections

The rotational behaviour of extended end plate connections can be predicted by means of the procedure suggested by Eurocode 3 in its Annex J [2]. The reliability of Annex J procedure for predicting the rotational behaviour of extended end plate connections has been statistically investigated by the authors [3,4,5] on the basis of comparison with a great number of experimental data collected in the technical literature [6-11]. In addition, some proposals have been developed to improve the codified approach leading to a better agreement with the experimental data.

Starting from these results, in order to stress the role of the main geometrical parameters defining the structural detail of extended end plate connections, a wide parametric analysis has been carried out [12].

The end plate of the analysed joints is extended at the beam tension flange side (Fig.1). At the tension flange level, the fastening action is assured by two bolt rows with two bolts for each row. Unstiffened joints (i.e. without continuity plates), both external and internal, have been considered by varying the column section, the beam section, the m/d ratio (Fig.1) (where d is the bolt diameter), the end-plate thickness and the bolt class.

In order to assure an adequate rotation capacity and to simplify the design procedure, the bolts have been designed to withstand the axial forces corresponding to a bending moment equal to 1.20 times the beam plastic moment.

Concerning the joint components affected by the state of stress of the column (column web in shear, column web in compression and column web in tension), some assumptions have been made. In particular, as the aim of the work [12] is to provide a design tool for detailing beam-to-column joints, simplified values of the coefficients taking into account the above state of stress have been considered [2]:

- the coefficient ξ taking into account the influence of the shear force in the column has been assumed equal to 1.0 in the case of external joints and equal to 0 in the case of internal joints, as suggested in Annex J;
- the coefficient k_{wc} taking into account the influence of the normal stress in the web (adjacent to the root radius), due to axial force and bending moment, has been assumed equal to 0.75, i.e. the most severe design condition has been considered.

In addition, as the aim of the work is to provide the designer with operative tools to quickly evaluate to joint resistance rather than the resistance of the joint-beam system, the limitation to the resistance given by the beam web and beam flange in compression has not been considered. This allows to classify the joints as full strength joints when the design

flexural resistance exceeds that of the connected member or as partial strength joints in the opposite case.

The flexural strength and the rotational stiffness of the examined joints have been computed by a modified version of Annex J, according to the authors' proposals [3,4,5].

The first outcome of this parametric analysis is the relationship between the rotational stiffness and the flexural resistance of joints. To this scope, it is useful to adopt the concept of equivalent beam length [13]. The equivalent beam length L_e represents the value of the beam length which corresponds to the equality between the joint rotational stiffness and the beam flexural stiffness:

$$K_\varphi = \frac{E I_b}{L_e} = \frac{E I_b}{\eta d_b} \tag{1}$$

where the equivalent beam length has been expressed as η times the beam depth d_b (where K_φ is the joint rotational stiffness and I_b is the beam inertia moment).

According to this definition, the parameter η can be used to represent the joint rotational deformability:

$$\eta = \frac{L}{d_b K} \tag{2}$$

where K is the nondimensional rotational stiffness of the joint, defined as the ratio between the joint rotational stiffness K_φ and the beam flexural stiffness EI_b/L (where L is the beam length). The parameter η can be conveniently used, because it provides through $1/\eta$ a nondimensional stiffness independent of the beam length as it is immediately recognized considering that $1/\eta = K_\varphi d_b/E I_b$.

In addition, the joint flexural resistance can be expressed through the nondimensional parameter:

$$\overline{M} = \frac{M_{j.Rd}}{M_{b.Rd}} \tag{3}$$

which represents the ratio between the design flexural resistance of the joint and that of the connected beam.

Starting from the consideration that the joint flexural resistance increases as the rotational deformability decreases and accounting for the results of a wide parametric analysis [12], the following mathematical structure has been chosen for the $\overline{M} - \eta$ relationship:

$$\overline{M} = C_1 \eta^{-C_2} \tag{4}$$

where C_1 and C_2 are two constants which can be computed by regression analysis.

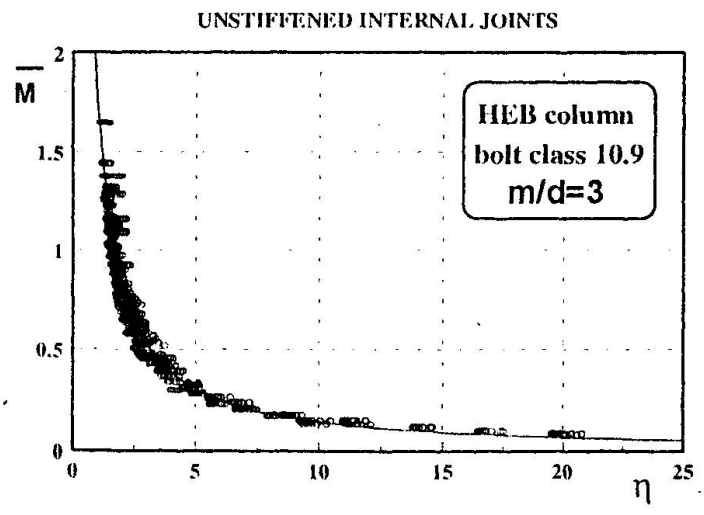

Fig.2 - $\overline{M} - \eta$ relationship for unstiffened internal joints and $m/d = 3$

The regression analyses of the results of the numerical simulations have confirmed the validity of the above relationship provided that the influence of the spacing between the bolts and the beam section is taken into account. In other words, it is possible to obtain a relationship of type (4) for any given value of the parameter m/d [12].

With reference to unstiffened internal joints, the relationship $\overline{M} - \eta$ is presented in Fig.2 for m/d=3, where the points represent the data of the numerical analyses. As an example, the coefficients C_1 and C_2, the

Table 1 - Coefficients of $M-\eta$ regressions (HEB columns, IPE beams, bolt class 10.9)

GROUP	m/d	C_1	C_2	n	r
UNSTIFFENED INTERNAL JOINTS	2	2.1421	1.6825	1239	0.91
	3	1.7691	1.0955	1463	0.97
	4	1.6080	0.8482	1309	0.98
	5	1.5167	0.7164	1232	0.98
UNSTIFFENED EXTERNAL JOINTS	2	3.6069	1.7982	1239	0.94
	3	2.2169	1.1569	1463	0.97
	4	1.8309	0.8817	1309	0.98
	5	1.6416	0.7351	1232	0.98

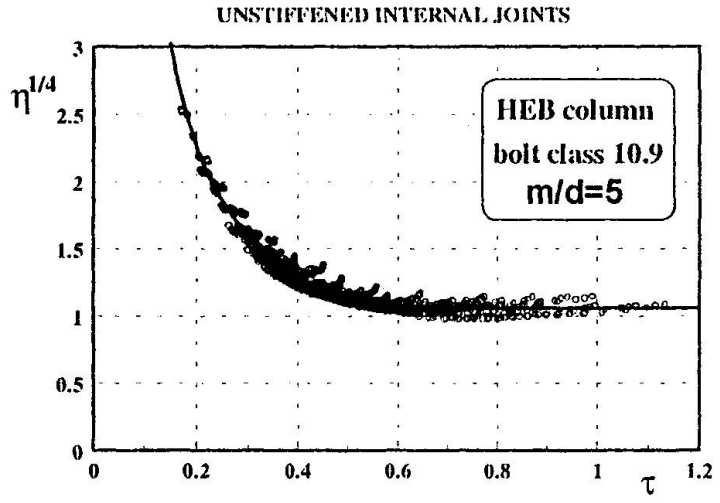

Fig.3 - $\eta-\tau$ relationship for unstiffened internal joints and $m/d=5$

correlation coefficient r and the data number n are given in Table 1 with reference to HEB columns, IPE beams and bolt class 10.9. The complete series of results for HEA and HEM columns and for bolt class 8.8 are presented in reference [12].

The correlation coefficients are always very close to 1 confirming the accuracy of the proposed relationship (4).

The examination of the failure modes of the designed extended end plate joints have evidenced that the column flange and the end plate in bending are generally involved [12]. Therefore, it can be stated that, for any given m/d ratio, the most important geometrical parameters governing the joint behaviour are the column flange thickness and the end plate thickness. For this reason, in order to account for the fact that the column flange in bending and the end plate in bending behave as a series of springs, the following parameter t_{eq} has been introduced:

$$\frac{1}{t_{eq}^3}=\frac{1}{t_{fc}^3}+\frac{1}{t_{ep}^3} \tag{5}$$

where t_{fc} and t_{ep} are the thicknesses of the column flange and of the end plate, respectively.

This parameter has been properly nondimensionalized according to the following relationship:

$$\tau=\left(t_{eq}^3\, d_b/I_b\right)^{1/4} \tag{6}$$

The relationship between the joint rotational deformability, expressed by means of the parameter η, and the thickness of the connected elements, expressed by τ, can be investigated through the numerical data of the parametric analysis.

Starting from the consideration that, obviously, the joint rotational deformability increases as the thickness of the connected elements decreases and from the observation of the numerical analysis data, the following mathematical structure has been selected for the $\eta-\tau$ relationship:

$$\eta^{0.25}=\frac{C_3}{\tau-C_4}+C_5\geq C_6 \tag{7}$$

Table 2 - Coefficients of $\eta - \tau$ regressions (HEB columns, IPE beams, bolt class 10.9)

GROUP	m/d	C_3	C_4	C_5	C_6	s	n
UNSTIFFENED INTERNAL JOINTS	2	0.081	0.035	0.850	1.128	0.032	1239
	3	0.172	0.024	0.655	1.111	0.043	1463
	4	0.248	0.027	0.535	1.089	0.047	1309
	5	0.310	0.029	0.459	1.054	0.056	1232
UNSTIFFENED EXTERNAL JOINTS	2	0.060	0.047	1.034	1.182	0.032	1239
	3	0.146	0.032	0.797	1.148	0.032	1463
	4	0.204	0.044	0.681	1.104	0.035	1309
	5	0.296	0.031	0.526	1.070	0.046	1232

where the coefficients C_3, C_4, C_5 and C_6 can be computed through a nonlinear regression by means of the least squares method.

With reference to unstiffened internal joints and to $m/d = 5$, the relationship $\eta - \tau$ and the corresponding data are presented in Fig.3, where the double square root of the parameter η has only been used to improve the readability of the figure. As an example, the coefficients C_3, C_4, C_5 and C_6 corresponding to HEB columns, IPE beams and bolt class 10.9 are given in Table 2 where the standard deviation s and the data number n are also presented. The complete series of results is given in reference [12] where HEA and HEB columns and bolt class 8.8 are also considered.

It is interesting to point out the physical meaning of the limitation provided to the connection deformability parameter η by the coefficient C_6. In fact, the influence of the joint components depending on the column section (i.e. the column web in shear, the column web in compression, the column flange in bending and the column web in tension) becomes more and more important as the end plate thickness increases. As a consequence, when the end plate thickness is sufficiently great so that its deformability is negligible, the joint deformability becomes almost constant being a feature of the beam-column coupling, of the m/d ratio and of the bolt class.

3. Design abaci

The results of the parametric analysis have pointed out that the behavioural parameters of extended end plate connections ($\overline{M}$, η), are strictly related. In addition, the deformability parameter η is strictly related to the parameter τ which accounts for the influence of the thickness of the connected elements.

From the design point of view, it has to be pointed out that, according to Annex J, nonlinearity arises before the design resistance of beam-to-column joints is completely developed (Fig.4). As, for economy, joints have to be designed to obtain a flexural resistance $M_{j,Rd}$ close to the design bending moment $M_{j,Sd}$, this means that elastic structural analyses can be carried out on the basis of the secant rotational stiffness of the joints [14], corresponding to $M_{j,Rd}$. According to Annex J, this secant stiffness is given by (Fig.4):

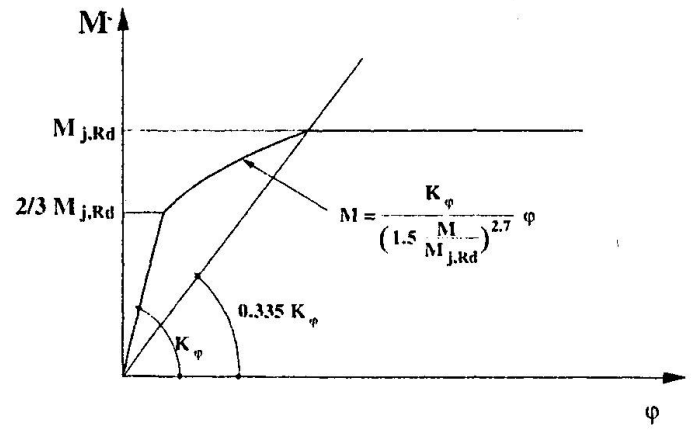

Fig.4 - Moment-rotation curve according to Annex J

$$K_{\varphi_{sec}} = 0.335\, K_{\varphi} \qquad (8)$$

The corresponding nondimensional secant rotational stiffness is given by:

$$K_{sec} = \frac{K_{\varphi_{sec}} L}{E I_b} = 0.335\, K \qquad (9)$$

Obviously, the corresponding secant deformability parameter can be defined according to the relationship:

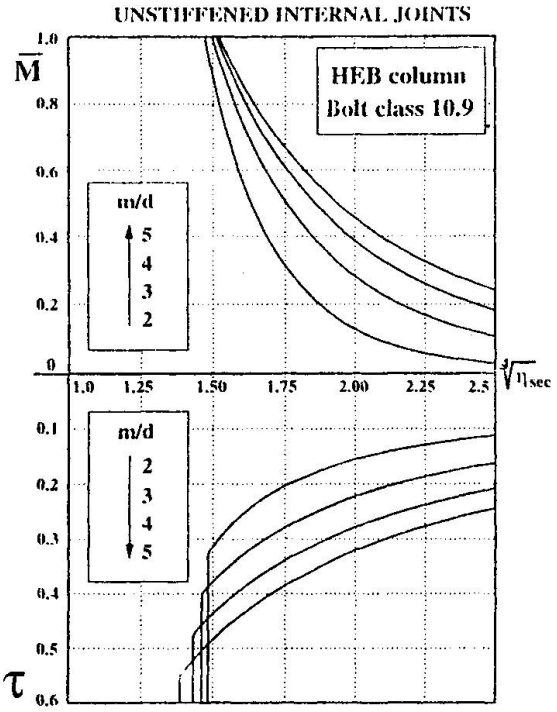

Fig.5 - Design abacus for unstiffened internal joints

$$\eta_{sec} = \frac{L}{d_b K_{sec}} = \frac{1}{0.335}\eta \approx 3\eta \qquad (10)$$

As the joint design has to be based on the secant stiffness $K_{\varphi sec}$, it is clear that, for design purposes, the previous correlations $\bar{M}$ versus η and η versus τ have to be rearranged using the secant deformability parameter η_{sec}.

The relationships obtained by the regression analyses provide the designer with an operative tool for detailing beam-to-column connections. In fact, for each group of joints, it is possible to provide the design abacus presented, as an example, in Fig. 5 where reference is made to the joint secant deformability parameter η_{sec}.

The structural analysis requires the knowledge of the joint rotational stiffness, whose value can be chosen on the basis of different design requirements such as the limitation of the beam deflections imposed by service conditions in braced frames. For a given beam and a given column, the lower part of the design abaci provides the end-plate thickness required to assure the desired value of the joint rotational stiffness, for different values of the m/d ratio. In addition, by means of the upper part of the abaci the flexural resistance of the joint can be evaluated as a function of the m/d ratio which, therefore, can be selected on the basis of the design internal actions obtained from elastic analysis.

However, it must be stressed that any design approach generally requires an iterative procedure, because the internal actions that joints have to withstand depend on the joint properties. A method to overcome this difficulty will be presented in Section 4 with reference to semirigid braced frames and uniform loads acting on the beams. The procedure can be easily extended to other loading conditions.

4. Design of braced frames

4.1 Design conditions

Braced frames are usually designed assuming that beams are pin-jointed to the columns. In other words, the beam-to-column joints are designed to transmit the shear forces only and the beams are designed to withstand a bending moment equal to $q_t L^2/8$, where q_t is the total vertical uniform load (including the partial safety factors, i.e. $q_t = 1.35\, g_k + 1.5 q_k$ where g_k and q_k are the characteristic values of the permanent and live load, respectively) acting on the beams whose span is L.

The use of semirigid joints, such as extended end plate connections, allows to reduce the maximum bending moment and the midspan deflection that the beam has to sustain so that a smaller section can be adopted.

The design procedure of braced frames can be based on a very simple model represented by a beam partially restrained at its ends. With reference to this model, five design conditions have to be taken into account. The first two conditions are the check of beam resistance against the sagging and hogging moment, respectively. Other two conditions concern the serviceability limit state requiring the limitation of the beam deflection under both live loads and total loads. The last design condition is the check of the resistance of the joints subjected to the hogging moments.

The check of the beam resistance against the sagging moment requires the fulfilment of the following relationship:

$$K_{sec} \geq \frac{6(1-\alpha)}{3\alpha - 1} \tag{11}$$

where:

$$\alpha = \frac{M_{b,Rd}}{q_l L^2/8} \tag{12}$$

The check against the hogging moment is given by:

$$K_{sec} \leq \frac{6\alpha}{2 - 3\alpha} \tag{13}$$

It is important to underline that both in equation (11) and in equation (13) reference has been made to the secant stiffness. This is justified taking into account that an economic design of joints requires a joint flexural resistance very close to the design hogging moment.

With reference to the serviceability limit state, according to Eurocode 3 [15], the maximum beam deflection under live loads has to be less than 1/350 times the beam span. This requirement can be expressed by the relationship:

$$K \geq \frac{2\beta_l}{1 - \beta_l} \tag{14}$$

The parameter β_l is given by:

$$\beta_l = \frac{5}{4} - \frac{f_l\, 96\, E\, I_b}{q_k L^4} \tag{15}$$

where q_k is the characteristic value of the uniform live load and $f_l = L/350$ is the limit deflection under live loads.

With reference to the secant stiffness, equation (14) gives:

$$K_{sec} \geq \frac{6\beta_l}{1 - \beta_l} \tag{16}$$

In addition, according to Eurocode 3 [15], the maximum beam deflection under the total loads has to be less than $f_t = L/250$. This design condition leads to the relationship:

$$K_{sec} \geq \frac{6\beta_t}{1 - \beta_t} \tag{17}$$

where:

$$\beta_t = \frac{5}{4} - \frac{f_t\, 96\, E\, I_b}{q_t L^4} \tag{18}$$

It must be stressed that the use of the initial nondimensional rotational stiffness K (instead of K_{sec}) in equation (14) is due to the reduced load levels for serviceability limit states (i.e in this case $q_l = g_k + q_k$) which leads to a significant reduction of the bending moment $M_{j,Sd}$. This justifies the use of the initial rotational stiffness of joints in evaluating the beam deflection.

Therefore, according to the first four design conditions, the nondimensional rotational stiffness of the joint has to be designed so that the secant stiffness lies in the range $K_{sec_{min}} - K_{sec_{max}}$ defined by:

$$K_{sec_{min}} = \max\left\{\frac{6(1-\alpha)}{3\alpha - 1}\ ;\ \frac{6\beta_l}{1 - \beta_l}\ ;\ \frac{6\beta_t}{1 - \beta_t}\right\} \tag{19}$$

$$K_{sec_{max}} = \frac{6\alpha}{2 - 3\alpha} \tag{20}$$

When the parameter α exceeds $\frac{2}{3}$ there is not any limitation to the joint rotational stiffness.

The last design condition regards the check of resistance of the joints. This condition defines the minimum strength that the joints have to develop, through the relationship:

$$\frac{q_t L^2/12}{M_{b.Rd}} \frac{K_{sec}}{K_{sec} + 2} \leq \overline{M} \tag{21}$$

which, through equations (12) and (10), gives:

$$\overline{M} \geq \frac{1}{3\alpha} \frac{2}{1 + \frac{2\eta_{sec}}{L/d_b}} \tag{22}$$

4.2 Design algorithm

The previous design conditions and the relationships relating the joint rotational behaviour to its geometrical parameters allow to develop a design algorithm which provides simultaneously the beam section and the geometrical parameters of the joints. The design algorithm is given by the following steps:

a) select the beam section, according to the most economical solution, to withstand a bending moment equal to $q_t L^2/16$ which corresponds to a nondimensional secant stiffness K_{sec} of the joint equal to 6;

b) as, in general, the design resistance of the selected beam section exceeds $q_t L^2/16$, compute the range of stiffness $K_{sec_{min}} - K_{sec_{max}}$, given by equations (19) and (20), and the corresponding range of the joint rotational deformability $\eta_{sec_{min}} - \eta_{sec_{max}}$ defined by:

$$\eta_{sec_{min}} = \frac{L}{d_b K_{sec_{max}}} \qquad \eta_{sec_{max}} = \frac{L}{d_b K_{sec_{min}}} \tag{23}$$

where $\eta_{sec_{min}} = 0$ when α exceeds 2/3.

c) for the selected m/d ratio, compute the coordinates $(\eta^*_{sec}, \overline{M}^*)$ of the point A (Fig.6) corresponding to the intersection between the continuous curve representing the flexural resistance which the joint is able to provide (i.e. equation (4) rearranged as $\overline{M} - \eta_{sec}$ taking into account that $\eta_{sec} \approx 3\,\eta$) and the dashed curve, given by equation (22), representing the design value of the bending moment (for a given α value). This figure refers to the practical application of the proposed design method, corresponding to the example given in the following Section;

d) control the location of the intersection point. If for the selected m/d ratio the intersection point is outside the range $\eta_{sec_{min}} - \eta_{sec_{max}}$ the joint cannot be designed for the chosen beam. In such a case, select the next beam section from the standard shapes and return to point b). On the contrary, if for a selected m/d ratio the intersection point lies within the above range, design the beam-to-column joints according to the following steps;

e) for the selected m/d ratio, compute the τ parameter which, according to equation (7), is given by:

$$\tau = \frac{C_3}{\eta^{0.25} - C_5} + C_4 \tag{24}$$

f) compute the parameter t_{eq} through equation (6);

g) for a given column section, compute the end plate thickness through equation (5) which provides:

$$t_{ep} = \frac{t_{eq}\, t_{fc}}{\left(t_{fc}^3 - t_{eq}^3\right)^{1/3}} \tag{25}$$

Equation (25) can be applied provided that $t_{fc} > t_{eq}$. If the above condition is not satisfied then select the next beam section from the standard shapes or, if any other design restraint exists, increase the column size and return to point b).

In fact, it is important to underline that, for a given beam section, the requirement $t_{fc} > t_{eq}$ shows that it is not always possible to design joints having a fixed rotational behaviour, i.e. strength and stiffness, with an arbitrary column section. This is justified by the fact that the

joint behaviour is also governed by some components depending on the column section. Typical cases are those of high beams which cannot be combined with small columns due to the collapse of one of the joint components belonging to the column.

5. Application

In order to show the practical application of the proposed procedure, the design of a braced frames has been developed and a comparison, from the economical point of view, between the solution with pin-joints (as an example double web angle connections) and that with semirigid joints is carried out.

The bay span of the examined frame is equal to 7.0 m and the interstorey height is equal to 3.5 m (Fig.8). All members are in Fe360 steel. The uniform loads acting on the beams are 28.5 kN/m and 19 kN/m for permanent and live loads respectively, including the partial safety factors equal to 1.35 and 1.5 respectively.

In the solution with pinned joints the beams have an IPE450 section, while the use of semirigid joints allows to reduce the beam section up to an IPE360. The beam-to-column joints have been designed according to the method previously described. Reference has been made to an m/d ratio equal to 2.

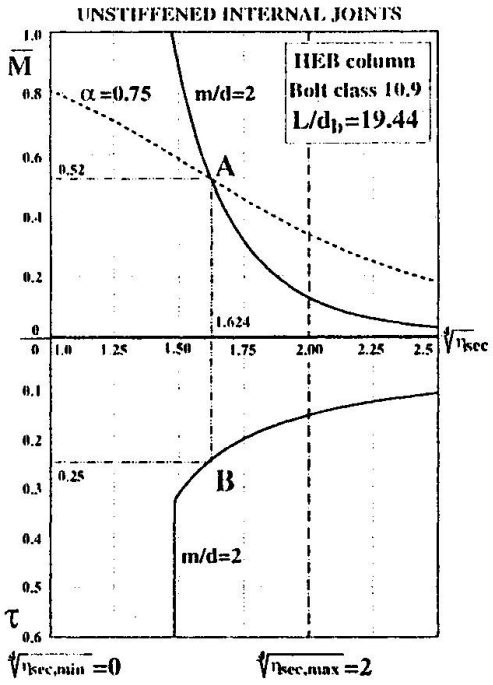

Fig.6 - Design procedure for braced frames

The graphical representation of the design procedure is given in the already mentioned Fig.6, with reference to internal joints. For the given loading condition and the selected beam (IPE360) the parameter α is equal to 0.75 and the required joint flexural resistance, as a function of the joint rotational deformability, is represented by the dashed curve. The intersection (A) with the continuous curve, representing for $m/d = 2$ the resistance that joint is able to develop, provides $\bar{M} = 0.52$ and $\eta_{sec}^{0.25} = 1.624$. This solution lies within the range defined by equations (23), being $\eta_{sec_{min}} = 0$ and $\eta_{sec_{max}} = 16$, therefore it satisfies resistance and deformability requirements. The value of the parameter τ defining the end plate thickness is equal to 0.25. For each column section, the corresponding minimum value of the required end plate thickness $t_{ep_{min}}$, computed through equations (6) and (25), is given in Fig.7 where the adopted design value t_{ep} is also shown. Furthermore, the design results concerning external joints, obtained with the same method, are also indicated. In addition, for each designed joint, this figure provides the values of the nondimensional secant and initial rotational stiffness (K_{sec} and K, respectively) and flexural resistance computed by the modified version [3,4,5] of Annex J for the adopted values of the end plate thickness.

On the basis of the computed joint rotational stiffness, the elastic analysis of the designed semirigid frame has been carried out and the stability and resistance of members has been checked according to Eurocode 3 [15].

With reference to the examined structural scheme, the use of semirigid joints has led to a significant economy in structural weight (18.1%).

6. Conclusions

In this paper, the relationships between the parameters describing the rotational behaviour of extended end plate connections, i.e. nondimensional strength and stiffness, have been

recalled evidencing how they can be predicted on the basis of some important geometrical parameters, such as the m/d ratio, the end plate thickness and the column flange thickness.

Starting from these results, effective design tools have been suggested and their use in a rational design procedure has been presented for braced frames. The innovative feature of the proposed design procedure consists in its ability to guide the designer up to the complete detailing of beam-to-column joints.

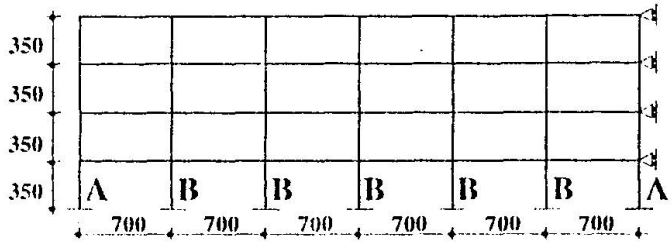

		PINNED	SEMIRIGID					
			profile	$t_{ep,min}$ (mm)	t_{ep} (mm)	K	K_{sec}	$\overline{M}$
COLUMNS	A	HE 180 B	HE 180 B	16.0	16	4.61	1.54	0.37
	B	HE 220 B	HE 220 B	14.0	15	8.98	3.01	0.59
BEAMS		IPE 450	IPE 360					
TOTAL WEIGHT		19.50 t	15.97 t (-18.10 %)					

Fig.7 - Application of the proposed design procedure and comparison with the pinned solution

Finally, the design example presented in this paper has shown the economical convenience of using semirigid joints. Taking into account that, as suggested by some authors [16], the increase of cost with respect to pinned frames due to the detailing of beam-to-column joints is about 5%, the economy, from the point of view of the overall cost of the structure, can reach 10% and more.

7. References

[1] SPRINT, European Community Strategic Programme for Innovation and Technology: «Steel Moment Connections according to Eurocode 3: Simple Design Aids for Rigid and Semirigid Joints», May, 1995.
[2] Eurocode 3, part 1.1: «Revised Annex J: Joints in Building Frames»
[3] C. Faella, V. Piluso, G. Rizzano: «Reliability of Eurocode 3 Procedures for Predicting Beam-to-Column Joint Behaviour», Third International Conference on Steel and Alluminium Structures, Istanbul, May, 1995.
[4] C. Faella, V. Piluso, G. Rizzano: «Proposals to improve Eurocode 3 Approach for Predicting the rotational Stiffness of Extended End Plate Connections», submitted for pubblication to Journal of Constructional Steel Research, June, 1995
[5] C. Faella, V. Piluso, G. Rizzano: «Some proposals to improve EC3-Annex J approach for predicting the moment-rotation curve of extended end plate connections», C.T.A., Italian Conference on Steel Construction, Riva del Garda, October, 1995.
[6] K. Weinand: «SERICON - Databank on joints in building frames», Proceedings of the 1st COST C1 Workshop, Strasbourg, 28-30 October.
[7] N. Kishi, W.F. Chen: «Database of Steel Beam-to-Column Connections», Structural Engineering Report, No. CE-STR-86-26, School of Civil Engineering, Purdue University, 1986.
[8] A.K. Aggarwal: «Comparative Tests on End Plate Beam-to-Column Connections», Journal of Constructional Steel Research, Vol. 30, 1994.
[9] P. Zoetemeijer, M.H. Kolstein: «Bolted Beam-Column Connections with Short End Plate», Report 6-75-20 KV-4, University of Technology, Delft, 1975.
[10] P. Zoetemeijer, H. Munter: «Extended End Plate with Disappointing Rotation Capacity: Test Results and Analysis», Report 6-75-20 KV-4, University of Technology, Delft, 1983.
[11] I. Simek, F. Wald: «Test Results of End Plate Beam-to-Column Connections», CTU, G-1121 Report, Prague, 1991.
[12] C. Faella, V. Piluso, G. Rizzano: «Design of Braced Frames with Extended End Plate Connections», Submitted for publication on Journal of Constructional Steel Research, January 1996.
[13] Bjorhovde R., Brozzetti J., Colson A.: «Classification System for Beam-to-Column Connections», Journal of Structural Engineering, ASCE, Vol.116, No.11, 1990
[14] Jaspart J.P., Briquet C.: «Sensitivity of Steel Building Frames to Joint Properties», International Colloquium on Stability of Steel Structures, Budapest, 1995
[15] Commission of the European Communities: «Eurocode 3: design of steel structures»,1990
[16] D. Anderson, A. Colson, J.P. Jaspart: «Connections and Frame Design for Economy», Costruzioni Metalliche, N.4, 1995.

Effective Length Factors in Precast Concrete Frames

Kim S ELLIOTT
Gwynne DAVIES
Halil GÖRGÜN
Department of Civil Engineering
University of Nottingham, UK

Drs Elliott (b 1953) and Davies (b 1935) are Senior Lecturer and Reader, respectively, in Structural Eng. Mr Görgün (b 1963) is a Research Student studying towards a PhD in this work. Drs Elliott and Davies have supervised some 8 projects in precast structures.

Summary

Column effective length factors β have been computed for a number of sway sub-frames in unbraced and partially braced precast concrete frames. The variable parameters were the number of semi-rigid connections in each of the sub-frames, the relative flexural stiffness α of the frame members, and the relative linear rotational stiffness K_s of the connection to that of an encastre beam. It is found that for values of $K_s < 2$ then β factors are more sensitive to changes in K_s than α. This is an important finding because experiments have shown that K_s to be less than 2 for typical sizes of beam. Parametric equations have been presented for the variations in β with K_s and α. The results enable designers to determine β factors for situations currently not catered for in codes of practice, in particular the upper storey of a partially braced frame.

1. Effective Length Factors in Column Analysis

The determination of column effective lengths in the analysis of reinforced concrete skeletal frames is well established and owes much to the work of Cranston (1), Wood (2), and Timoshenko et al (3). The notion of using effective length factors β to assess the buckling capability of a column, either individually or as part of a structural frame, has found favour with design engineers. Simple equations for β have been presented in terms of column end boundary conditions and/or relative frame stiffness functions, so that the designer may compute, not only column buckling capacities but also second order deflections and ultimate second order bending moments, often termed M_{add} (See Appendix). The British Code for concrete structures, BS 8110:1985 (4) has adopted such an approach after Cranston (1) whereby column end conditions were equated to α, the total relative stiffness of the column to that of the beam(s) (or beams and slabs) framing into the ends of the column. The approach may be used for both braced and unbraced concrete frames. The beam - column connections are assumed to be fully rigid and of equal (or greater) strength to that of the members.

Precast concrete skeletal frames, Fig. 1, are designed using pinned-jointed connections between columns, beams and floor slabs. The stability of an unbraced frame is therefore provided only by the cantilever action of the columns at the foundation because transfer of bending moments into the beams or slabs is not permitted. In determining β, BS 8110 allows a precast concrete frame to be analysed as though it were a rigid framework but with $\alpha = 10$. With the wide range of different types of beam - column connections used in precast frames, this arbitrary approach is neither rational nor representative of real behaviour, as previous and present full scale testing of connections in precast frames by the authors (5,6) and by Mahdi

(7) has shown. Although the rotational stiffness of the connections and the degree of semi-rigidity, defined by K_s = joint stiffness J / beam flexural stiffness 4EI/L, varies over a very wide range, there is clearly scope for the implementation of β factors which incorporate **both** the flexural responses of the frame and of the semi-rigid connections.

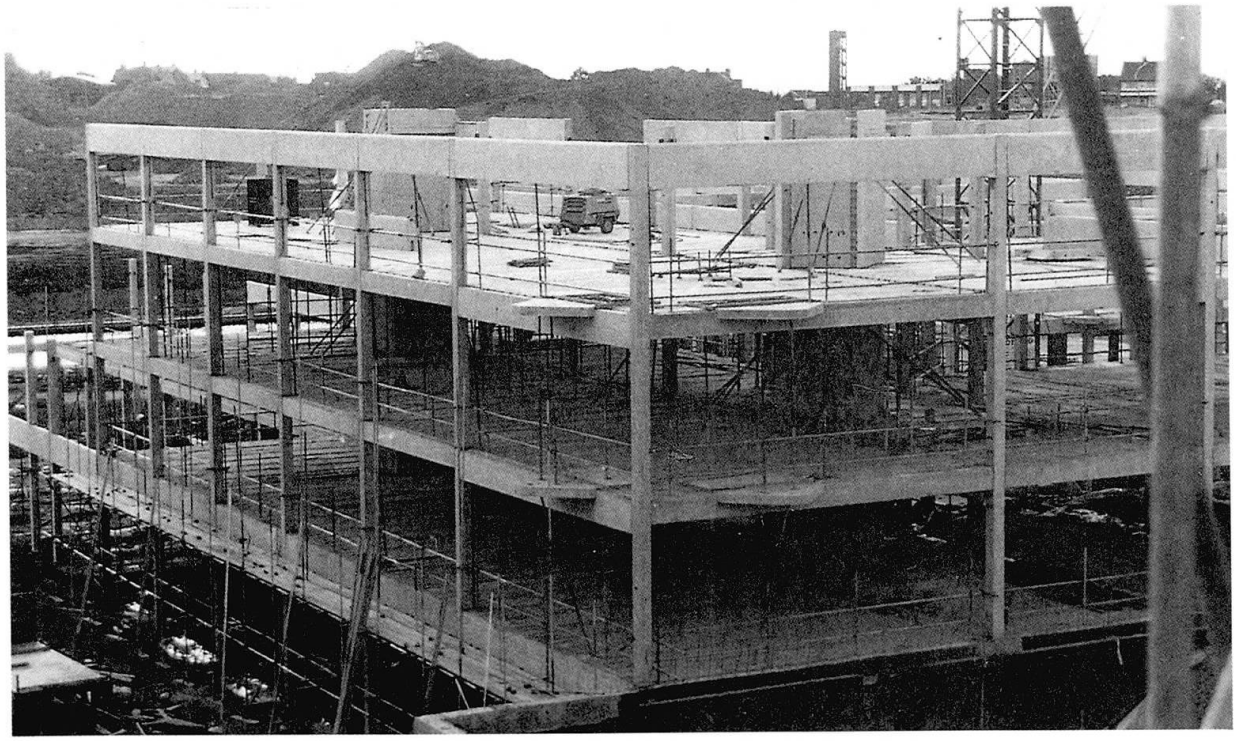

Fig. 1. Typical precast concrete skeletal frame.

In the context of the present work, *stability* implies general *frame stability* in which columns will not buckle independently of one another. It is therefore necessary to investigate the stability of a framework as a whole and to take into account α effects at both ends of the column. This paper presents the results for column effective length factors in three types of sub-frames commonly occurring in precast skeletal frames. Only sway frames are considered in this work. This instability was obtained using a geometric second-order computer program analysis developed by Aksogan and Görgün (8). In all cases maximum column loads in each sub-frame, and hence β factors are obtained for given values of α and K_s.

2. Parametric Study

Precast concrete sway frames are analysed either as *fully unbraced* frames, Fig. 2(a), or as *partially braced* frames, Fig. 2(b), where shear walls (or cores) provide lateral bracing up to a certain level and the frame is unbraced above this point.

Three sub frames, labelled F1, F2 and F3 in Fig. 2, were identified for the analysis. Sub frames F1 and F2 represent the upper floor and the ground floor levels, respectively, in an unbraced frame, whilst sub frame F3 represents the upper floor in a partially braced frame immediately above the level of the bracing. It may be seen in Fig. 2(b) that the columns adjacent to the bracing walls are fully encastre at their upper end, and may therefore be considered fully rigid at their lower end in the sub frame F3. In all cases the semi-rigid connections are positioned at the ends of the beams, reflecting the true nature of precast

skeletal frames having continuous columns (Fig. 1).

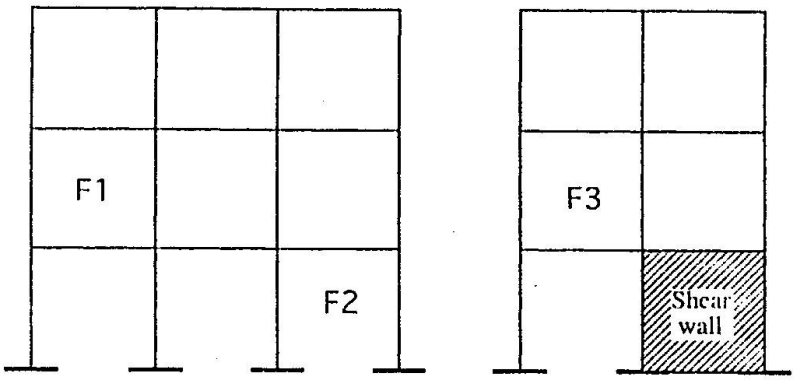

Fig. 2. Types of precast frames (a) unbraced (left) and (b) partially braced.

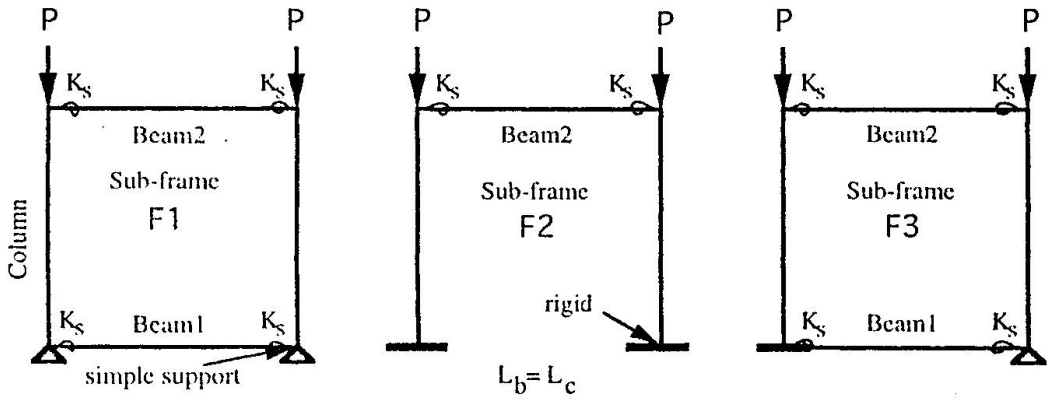

Fig. 2(c). Definitions of sub-frames used in the analysis.

The linear - elastic degree of semi-rigidity of the beam-column connections was specified as follows:

$K_s = 1 \times 10^{-9}$; to simulate a pinned-joint;
$1 \times 10^{-9} < K_s < 10$; to simulate a semi-rigid joint;
$K_s = 1 \times 10^{9}$; to simulate a fully rigid joint.

For the semi-rigid analysis, the range of values for α and K_s was obtained from realistic joint values used in typical precast concrete frames, i.e. $\alpha = 0.5$ to 2.0, and from the experimental test results for $K_s = 0$ to 10, but with a greater emphasis on the range $K_s = 0.1$ to 2.0. (In fact because the computer program requires a value for α greater than 0, $\alpha = 0.001$ was used to simulate $\alpha = 0$, and the minimum value of K_s for sub-frame F1 is 0.1 because this frame is unstable for $K_s = 0$.) For simplicity and reliability in the analysis, the length of the beams and columns in the sub-frames were made equal, and in general the cross sectional properties of the column members were varied in order to necessitate a change in α, although this is not important once the results are normalised with respect to α and β. The maximum critical load for the column converged to within an accuracy of better than 0.1 per cent of the ultimate squash load for the column, so that the error in β is approximately 0.1 per cent.

3. Results

3.1 Variations in Column Effective Length Factors for Rigid Connections

Comparing the results obtained from this work and those calculated using BS 8110 equations (see Appendix), Fig. 3 presents the results for the variation in β with α assuming fully rigid connections. Note that in the case of sub-frame F1, $\alpha_1 = \alpha_2$, where α_1 and α_2 are the relative stiffnesses of the column to the lower and upper beams, respectively. In sub-frame F2, $\alpha_1 = 0$ because the foundation is rigid. There is no equation in BS 8110 to deal with sub-frame F3.

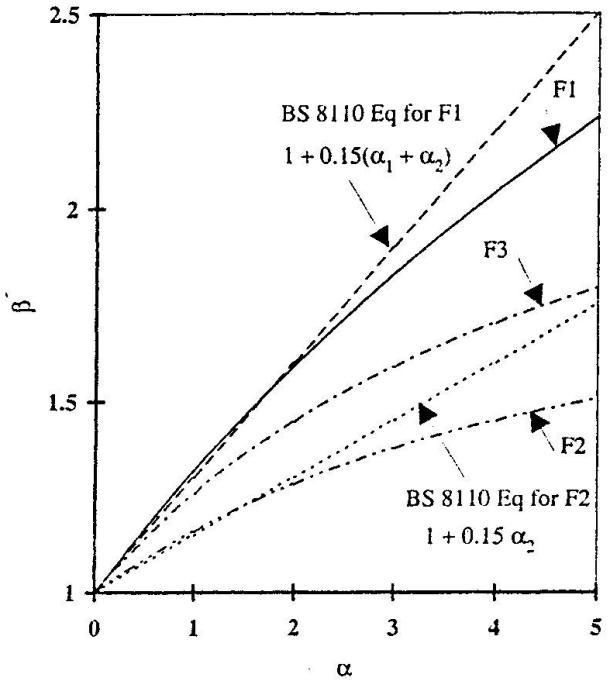

Fig. 3. Variation in column effective length factor β with frame stiffness α for rigid joints.

The results in Fig. 3 show that the code equations are in good agreement with analytical results for $0 < \alpha < 2$, and conservative thereafter. It is postulated that an equation for sub-frame F3 may be taken as the mean of the equations for F1 and F2. The results suggest that the code equations might be modified for values of $\alpha > 3$.

3.2 Variations in Column Effective Length Factors for Semi-Rigid Connections

Figs. 4 and 5 show the results for the variations in β with K_s for selected values of α in the upper storey sub-frame F1. Although a mapping function is required to demonstrate the full parametric variations, the three selected values for α show the trends clearly. The results in Fig. 4 show that for values of $K_s > 2$ or 3 the change in β is no more than about 5 per cent of its fully rigid value. For this reason Fig. 5 is an enlargement of Fig. 4 for values of $K_s < 2$. The dashed lines show the plots of the proposed parametric equations given in Section 3.3.

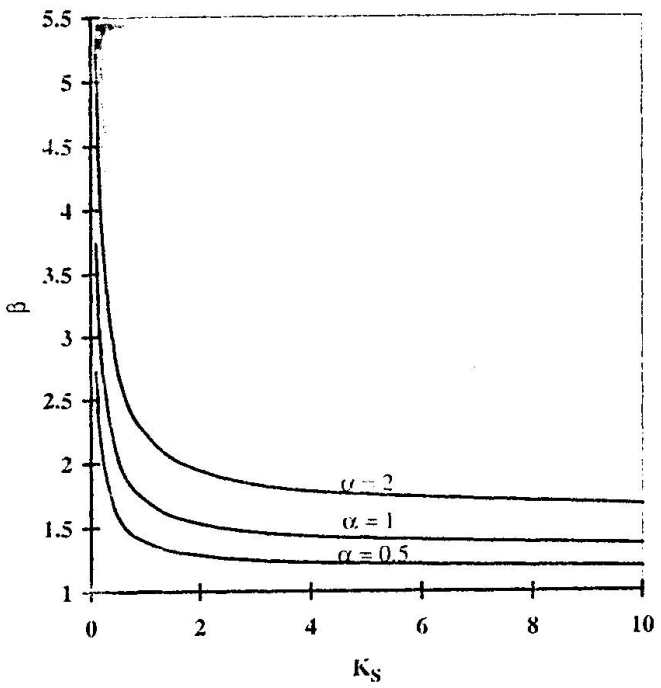

Fig. 4. *β factors vs $K_s \leq 10$ for selected values of α in sub-frame F1.*

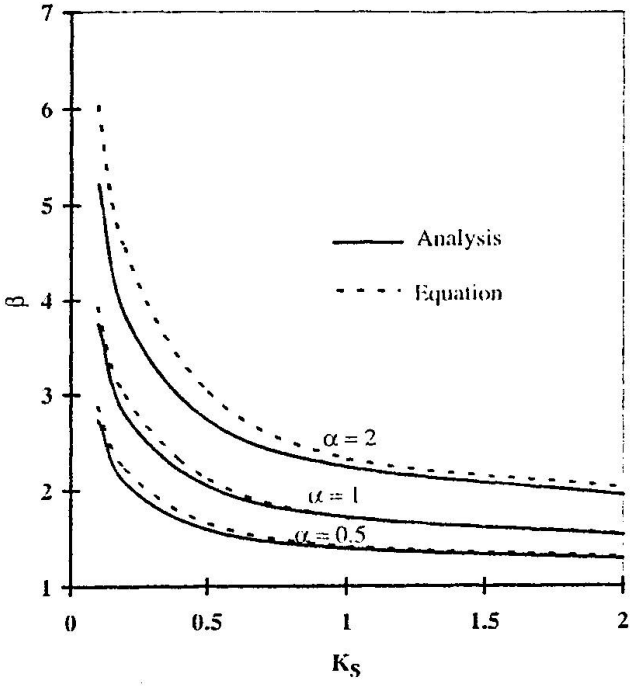

Fig. 5. *β factors vs $K_s \leq 2$ for selected values of α in sub-frame F1.*

Figs. 6 and 7 show similar sets of results for the same selected values of α for sub-frames F2 and F3, respectively. Results are presented only for values of $K_s \leq 2$ for the reasons outlined above. As expected the values of β in the ground floor sub-frame F2 converge at β = 2.0, and are independent of α. The corresponding value in sub-frame F3 is β = 2.7. A major difference between the upper floor (F3) the ground floor (F2) sub-frames is the more rapid decrease in β with K_s in the upper floor sub-frame. This is because F3 contains four semi-rigid connections,

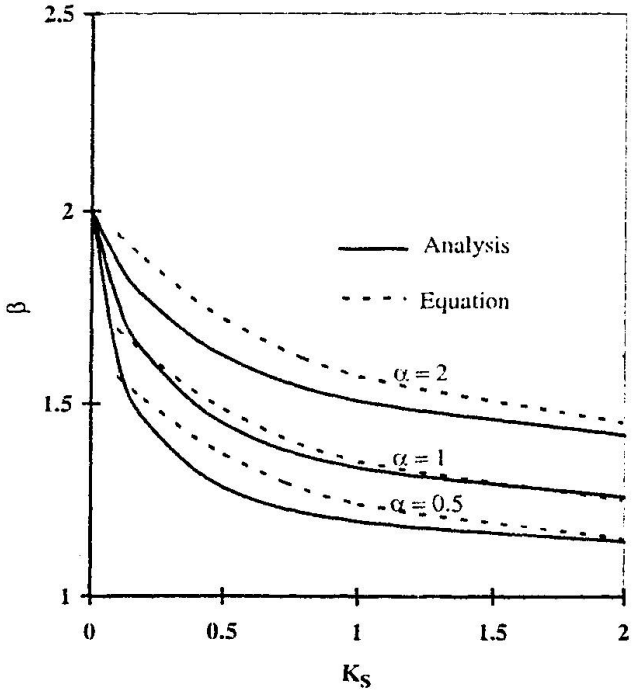

Fig. 6. *β factors vs $K_s \leq 2$ for selected values of α in sub-frame F2.*

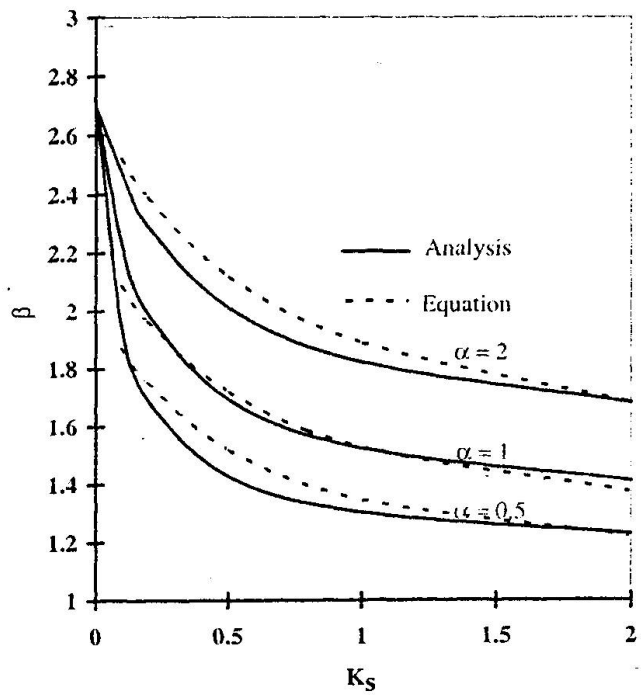

Fig. 7. *β factors vs $K_s \leq 2$ for selected values of α in sub-frame F3.*

(although one of them is located adjacent to a rigid column foundation) whereas F2 contains only two. Also, F3 has eight degrees of freedom whereas F2 has only six. This result has obvious implications for frameworks containing a small number of bays in the plane of bending, say 2 or 3, where the number of semi-rigid connections is disproportionately large to the number of columns. The variation in α does not appear to have any major influence on the behaviour of the various sub-frames once the effects of changes in K_s have been removed.

3.3 Parametric Equations

Subtracting the value of 1.0 from all the data and normalising the results with respect to α, the variation in $1/\beta$ with K_s is primarily linear and marginally quadratic. A simple analysis of a right angled knee-joint (comprising one beam and one column connected by a semi-rigid rotational spring) will show that the effect of the semi-rigid connection is to modify the relative stiffness of the members from α to α' where

$$\alpha' = \alpha \left(1 + \frac{1}{K_s} \right) \qquad [1]$$

For example if $\alpha = 0.5$ and $K_s = 0.6$ (say), then the effect of incorporating a semi-rigid connector is to increase the apparent stiffness of the column to $\alpha' = 1.33$, thus increasing β according to the results in Fig. 3. Thus the influence of the connector stiffness K_s is paramount in the present parametric equations, whilst that of α is of lesser influence over the range studied. The influence of K_s on β is greater for values of $K_s < 2$ than when $K_s > 2$, and therefore separate equations are presented to cater for the differences in behaviour at these points.

Referring to Figs. 4 and 5, the data for the upper storey sub-frame F1 may be approximated by using the following empirical relationship:

$$\beta = 1 + \frac{1}{0.2 + 10.0K_s} + \frac{\alpha}{0.3 + 1.8K_s - 0.45K_s^2} \quad \text{for } 0.1 < K_s \leq 2 \qquad [2]$$

$$\beta = 1.1 + \frac{1}{7.4 + 7.4K_s - 0.4K_s^2} + \frac{\alpha}{1.6 + 0.3K_s} \quad \text{for } 2 \leq K_s \leq 10 \qquad [3]$$

Thus, $\alpha = 0.5$ and $K_s = 0.6$ for example, equation [2] gives $\beta = 1.50$. If the value for the equivalent stiffness from Eq 1. ($\alpha' = 1.33$) is used in the BS 8110 equation, then $\beta = 1.40$. This shows that equating a semi-rigid connection to a rigid connection in an equivalent frame under estimates β for these particular parameters.

Referring to Fig. 6, the data for the ground floor sub-frame F2 may be given as:

$$\beta = 1 + \frac{1}{2.0 + 2.0K_s + 4.0K_s^2} + \frac{\alpha}{4.0 + 0.5K_s} \quad \text{for } 0.1 < K_s \leq 2 \qquad [4]$$

And for values of $K_s > 2$ not presented in the figures:

$$\beta = 1 + \frac{1}{8.6 + 8.4K_s - 0.4K_s^2} + \frac{\alpha}{3.9 + 0.9K_s} \quad \text{for } 2 \leq K_s \leq 10 \qquad [5]$$

Referring to Fig. 7, the data for the upper storey sub-frame F3 may be given as:

$$\beta = 1 + \frac{1}{1.25 + 2.5K_s + 2.5K_s^2} + \frac{\alpha}{2.25 + 0.5K_s} \quad \text{for } 0.1 < K_s \leq 2 \qquad [6]$$

And for values of $K_s > 2$ not presented in the figures:

$$\beta = 1 + \frac{1}{6.5 + 5.6K_s - 0.3K_s^2} + \frac{\alpha}{2.7 + 0.3K_s} \quad \text{for } 2 \leq K_s \leq 10 \qquad [7]$$

4. Discussion

It has been established that where column effective length factors β are determined within a structural framework, the nature of that framework and its boundary conditions will influence the results. All the results show an increase in β with:

i) an increasing number of degrees of freedom, and an increasing number of connections per sub-frame
ii) an increase in α
iii) a decrease in K_s.

In the context of precast concrete frame connections, where full scale experimental results indicate values of K_s between 0.2 and 2.0 [5,6,7] it is significant that for values of $K_s < 2$ the influence of connection stiffness on β is much greater than that of the relative stiffness of the frame members, particularly in sub-frame F1 where all connections are semi-rigid (see Fig. 4 and eq. 2 and eq. 3). In the sub-frames comprising at least one rigid foundation (i.e. F2 and F3) the variation in β with K_s and α is about equal for $K_s < 1$, and more dependent on α for $K_s > 1$. It is therefore concluded that maximum benefit in obtaining reductions in β with greater connection stiffness will accrue in upper storey sub-frames where $K_s < 1$, and in the ground floor sub-frame where $K_s < 0.5$.

The results obtained for the upper storey in the partially braced sub-frame F3 are of particular interest to designers because the boundary conditions for the column which is not adjacent to a shear wall is unspecified in codes of practice. Treating the column alone would lead to very high β factors and an impossible design situation (which can be appreciated from the design rules given in the Appendix). A pinned jointed frame can be idealised as shown in Fig. 8. In Fig. 8[a] the deflected profile of a column held in position but not in direction at level N, and a free cantilever above this level will have a β factor of at least 3.0 (assuming equal storey heights). However the true manner of slenderness induced deflections would be as shown in Fig. 8[b] where the effective length of *all* columns is 2.7. The restoring force in the beam is small but very significant in terms of frame stability. Bending moments resulting from sway in the unbraced part are carried over into the braced part of the frame, diminishing to zero with distance to the level of the floor below, such that β for the columns in the lower braced regions may be taken as 1.0.

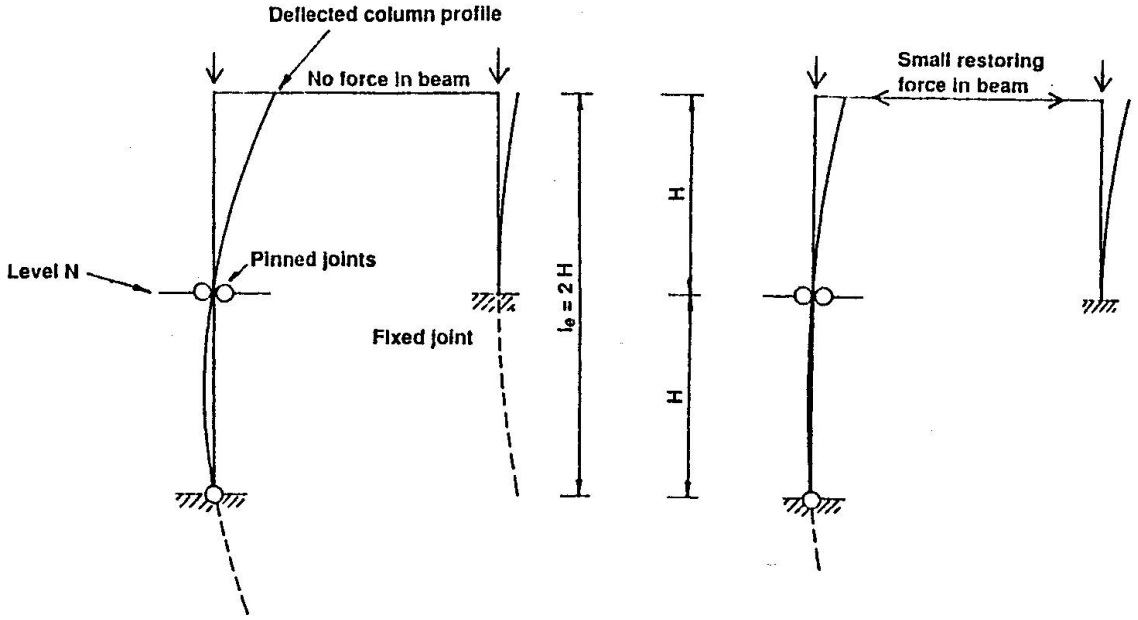

Fig. 8. Behaviour of a partially braced frame, (a) discrete column deflection profiles (left), (b) column deflection profiles in a frame environment (right).

5. Conclusions

Frame stability analyses on three types of one-storey x one-bay sub-frames in *unbraced* and *partially braced* precast concrete skeletal frames have shown that column effective length factors β increase due to:

i) an increasing number of total degrees of freedom at the connections in the ends of the beams. This is a direct measure of the number of semi-rigid connections per column, and is influenced by the location of the connections in the sub-frame;

ii) an increase in α, the relative stiffness of the columns to the beam members;

iii) a decrease in K_s, the relative stiffness of the connection to a fully encastre beam member. The influence of K_s on β is considerably greater for values of $K_s < 2$ than when $K_s > 2$.

Parametric equations have been presented for the variations in β with K_s and α. There are significant differences in the equations for values of K_s less than or greater than 2. For $K_s > 2$ the change in β is no more than about 5 per cent of its fully rigid value.

The results enable designers to determine β factors for situations currently not catered for in codes of practice, in particular the upper storey in a partially braced frame.

References

1. Cranston, W. Analysis and Design of Reinforced Concrete Columns, Research Report 20, Cement & Concrete Association, Wexham Springs, Aug. 1972.

2. Wood, R. H. Effective lengths of columns in multi-storey buildings, Parts 1, 2 and 3, The Structural Engineer, Vol. 52, Nos. 7, 8 and 9, July, Aug., Sept. 1974.

3. Timoshenko, S. and Gere, J. M. Theory of elastic stability, McGraw-Hill, 2nd. ed., 1961.

4. British Standards Institute, Structural Use of Concrete, BS 8110, London, 1985.

5. Elliott, K. S., Davies, G. and Mahdi, A. A. Semi-rigid joint behaviour on columns in precast concrete buildings, COST C1 Proceedings of the 1st Workshop, Semi-rigid Behaviour of Civil Engineering Structural Connections, E.N.S.A.I.S., Strasborg, Oct. 1992, p 282 - 295.

6. Görgün, H. Semi-rigid behaviour of connections in precast concrete structures, Dept. of Civil Engineering Report No. SR 96-001, University of Nottingham, Feb. 1996, 344 pp.

7. Mahdi, A. A. Moment rotation effects on the stability of columns in precast concrete structures, PhD thesis, University of Nottingham, 1992.

8. Aksogan, O. and Görgün, H. The nonlinear analysis of planar frames composed of flexurally connected members, Cukurova University Journal, Faculty of Engineering and Architecture, Vol. 8, No. 2, Dec. 1993, p117-129.

Appendix. Design Rules in BS 8110 for Columns in Unbraced Frames

β factors in Part 2, clause 2.5 for columns in frames may be taken as the lesser of:

$$\beta = 1.0 + 0.15\ (\alpha_{c1} + \alpha_{c2})$$

$$\beta = 2.0 + 0.3\ \alpha_{cmin}$$

where α_{c1} *= ratio of the sum of the column stiffnesses to the sum of the beam stiffnesses at the lower end of a column,*

α_{c2} *= ratio of the sum of the column stiffnesses to the sum of the beam stiffnesses at the upper end of a column,*

α_{cmin} *= lesser of* α_{c1} *and* α_{c2}

In the calculation of α_{cmin}, α_{c1} *and* α_{c2}, *only members properly framed into the end of the column in the appropriate plane of bending should be considered. In specific cases of relative stiffness the following simplifying assumptions may be used:*

(b) simply-supported beams framing in to a column: α_c *to be taken as 10;*

(c) connection between column and base designed to resist only nominal moment: α_c *to be taken as 10;*

Deflection induced moments in solid slender columns, BS 8110, Part 1, clause 3.8.3.
... account has to be taken of the additional moment induced in the column by its deflection.

This may be taken as $M_{add} = N(\beta l_o/b)^2 K h/2000$, *where* N = *ultimate axial load,* l_o = *clear height,* K = *a reduction factor that corrects the deflection to allow for the influence of axial load,* h = *overall depth of a column in the plane considered, and* b = *smaller dimension of a column.*

Acknowledgement

The authors wish to thank EPSRC and The Turkish Government for financial support. The computer program was developed with the assistance of Professor O Aksogan at Cukurova University, Turkey.

PLASTIC DESIGN OF SEMIRIGID FRAMES FOR FAILURE MODE CONTROL

Federico M. Mazzolani
Department of Structural Analysis and Design, University of Naples, Italy

Federico M. Mazzolani is Full Professor of Structural Engineering at the University of Naples (Italy). Author of more than 350 papers and 12 books in the field of metal structures, seismic design and rehabilitation. Member of many national and international organizations. Presently Chairman of: UNI-CIS/SC3 Steel and Composite Structures, CNR Fire Protection, ECCS-TC13 Seismic Design and CEN-TC250/SC9 Aluminium Alloy Structures.

Vincenzo Piluso
Department of Civil Engineering, University of Salerno, Italy

Vincenzo Piluso, born 1962, graduated in Civil Engineering in 1987 from the Naples University (Italy) where also received his PhD degree in Structural Engineering in 1992. Full member and secretary of ECCS TC13 on Seismic Design and member of COST C1 Seismic Working Group, presently he is researcher at the Department of Civil Engineering of Salerno University. His activity is mainly devoted to steel structures and seismic engineering.

Summary

A new method for the plastic design of moment resisting frames with semirigid connections is presented in this paper. The method is the extension to the case of semirigid frames of a procedure for the failure mode control already proposed by the authors with reference to rigid frames with full-strength beam-to-column connections. Starting from the analysis of the typical collapse mechanisms of frames subjected to horizontal forces, the method is based on the application of the kinematic theorem of plastic collapse. The beam section and the connection details are preliminary designed to resist vertical loads. As a consequence, the unknowns of the design problem are the column sections. They are determined by means of design conditions expressing that the kinematically admissible multiplier of the horizontal forces corresponding to the global mechanism has to be the smallest among all kinematically admissible multipliers. The preliminary design of beams and connections can be accepted provided that checks against the serviceability limit states are satisfied. Therefore, the complete design procedure includes also an iterations to fulfil serviceability requirements. In addition, second order plastic analysis is applied to account for the influence of P-Δ effects through linearized mechanism equilibrium curves.

1. Introduction

The simple design criteria, suggested by modern seismic codes, do not always lead to structural schemes failing in global mode. For this reason, a more sophisticated design procedure, assuring the development of a collapse mechanism of global type, has been recently proposed [1,2,3] and its reliability has been verified on a large number of structural schemes, leading in all cases to the fulfilment of the design requirement [4].

The method is based on the observation that the collapse mechanisms of frames under horizontal forces can be considered belonging to three main typologies (Fig.1). The collapse mechanism of the global type is a particular case of type-2 mechanism. The control of the failure mode can be performed through the analysis of $3n_s$ mechanisms (where n_s is the number of storeys). It is assumed that the beam sections and beam-to-column connections are preliminary designed to resist vertical loads. With reference to extended end plate connections, this preliminary design can be carried out through the procedure suggested in reference [5,6] which is able to guide the designer up to the complete detailing of beam-to-column joints. As a result of this preliminary design, only the column sections have to be determined. Aiming at the failure mode control, the values of the plastic section modulus of columns have to be defined so that the kinematically admissible multiplier of the horizontal forces corresponding to the global mechanism is less than those corresponding to the other

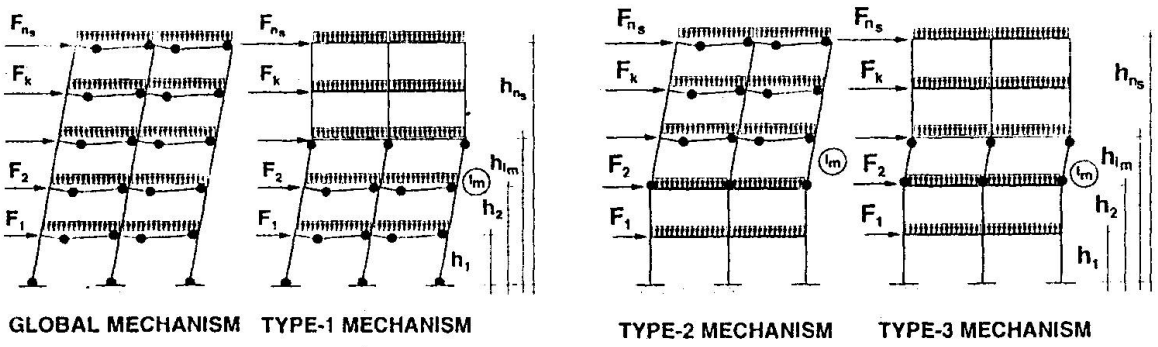

Fig.1 - Analysed collapse mechanism typologies

$3n_s$-1 kinematically admissibile mechanisms. It means that, according to the upper bound theorem, the above stated multiplier is the true collapse multiplier and, therefore, the true collapse mechanism is the global failure mode.

The results of the above design procedure, oriented only to the failure mode control, can be accepted provided that the checks against serviceability limit states are satisfied. In the opposite case, the rotational stiffness of beam-to-column joints or the beam sections have to be increased and the design procedure for failure mode control has to be repeated. Convergence is achieved when both failure mode control and fulfilment of serviceability requirements are obtained.

2. Location of plastic hinges in beams with semirigid connections

The rotational stiffness and the flexural resistance of beam-to-column joints are strictly related. In particular, this has been evidenced with reference to extended end plate connections showing how, decreasing the joint rotational deformability, the joint flexural resistance increases [5,6]. Therefore, depending on the structural detail of the connection, semirigidity can lead to full-strength or to partial-strength joints. In the first case, yielding is located at the member ends so that plastic hinges develop the beam plastic moment. On the contrary, in the second case, yielding occurs in the connecting elements so that plastic hinges develop the joint flexural resistance whose magnitude is less than the beam plastic moment. However, it is important to stress that the location of the plastic hinges depend on the magnitude of vertical loads acting on the beams as well as on the degree of flexural resistance of the beam-to-column connections. In the following, for seak of simplicity, reference will be made only to the case of uniform loads acting on the beams. The results for other beam loading conditions can be similarly derived.

In addition, the case of non-proportional loading will be considered, because failure mode control assumes primary importance in seismic design. The seismic action is modelled through a system of horizontal forces whose distribution can be selected according to a proper combination of the eigenmodes. The magnitude of these horizontal forces is governed by the multiplier α, while the vertical loads are assumed to be constant. For this reason, at any loading stage characterized by a given value of the horizontal force multiplier α, the bending moment diagram of the beams is the result of the superposition of those due to both vertical and horizontal forces. It means that, increasing the horizontal forces (i.e. the multiplier α), the first plastic hinge is always developed at the beam end or the con-

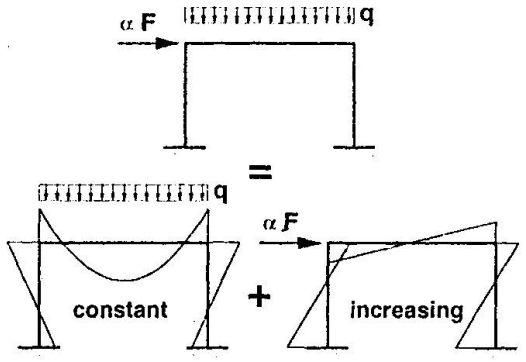

Fig.2 - Plastic hinge location

nection opposite to the horizontal forces (Fig.2).

Regarding the location of the second plastic hinge, it is strictly dependent on the magnitude of vertical loads and on the flexural resistance of connections.

The flexural resistance of connections is expressed through the following nondimensional parameters:

$$\overline{m}_l = \frac{M_{j.Rd}^{(left)}}{M_b} \qquad \overline{m}_r = \frac{M_{j.Rd}^{(right)}}{M_b} \tag{1}$$

where $M_{j.Rd}^{(left)}$ and $M_{j.Rd}^{(right)}$ are the design flexural resistance of left and right beam-to-column joints, respectively; M_b is the design plastic moment of the beam section.

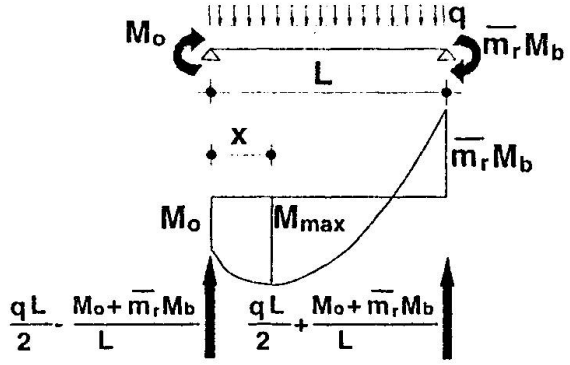

Fig.3 - Analysis of plastic hinge location

The location of plastic hinges can be determined taking into account that the plastic moment $\overline{m}_r M_b$ acts at one end, where the first plastic hinge is formed, while at the second end there is a bending moment M_o which progressively increases due to the progressive increase of the horizontal forces (Fig.3). The maximum bending moment is attained at the abscissa given by:

$$x = \frac{L}{2} - \frac{M_o + \overline{m}_r M_b}{q\,L} \tag{2}$$

where L is the beam length and q is the uniform load acting on the beam.

The maximum bending moment, which occurs at the abscissa provided by equation (2), is given by:

$$M_{max} = \frac{M_o - \overline{m}_r M_b}{2} + \frac{q\,L^2}{8} + \frac{(M_o + \overline{m}_r M_b)^2}{2\,q\,L^2} \tag{3}$$

It can be observed that the second plastic hinge can develop in an intermediate beam section provided that the yielding condition $M_{max} = M_b$ and the limitation $M_o < \overline{m}_l M_b$ are contemporaneously satisfied. The yielding condition $M_{max} = M_b$ gives, through equation (3), a second order equation whose positive solution is given by:

$$M_o = \left[2\,M_b\,q\,L^2\,(\overline{m}_r + 1)\right]^{1/2} - \overline{m}_r M_b - \frac{q\,L^2}{2} \tag{4}$$

which represents the value of the end moment M_o corresponding to the occurrence of the second plastic hinge at the abscissa provided by equation (2).

By imposing the limitation $M_o < \overline{m}_l M_b$, a limit value is found for the magnitude of the vertical load acting on the beams:

$$q > \frac{2\,M_b}{L^2}\left\{(2 + \overline{m}_r - \overline{m}_l) + 2\left[(\overline{m}_r + 1)(1 - \overline{m}_l)\right]^{1/2}\right\} \tag{5}$$

which, in the case of full-strength joints, provides $q > 4\,M_b/L^2$.

This means that the second plastic hinge develops in an intermediate beam section provided that relationship (5) is satisfied. In the opposite case, the two beam ends or connections are involved.

The abscissa of the intermediate section where the second plastic hinge forms, provided that condition (5) is satisfied, can be computed by combining equation (4) with equation (2). This gives:

$$x = L - \left(\frac{2\,M_b\,(\overline{m}_r + 1)}{q}\right)^{1/2} \tag{6}$$

where, obviously, the limit case of full-strength joints is obtained for $\overline{m}_r = 1$.

3. Second order plastic analysis

3.1 Notation

The following notation is adopted:

- n_s is the number of storeys;
- n_c is the number of columns;
- n_b is the number of bays;
- k is the storey index;
- i is the column index;
- j is the bay index;
- i_m is the mechanism index;
- L_j is the span of the jth bay;
- $M_{c,ik}$ is the plastic moment, reduced for the presence of the axial internal force, of the ith column of the kth storey;
- $M_{b,jk}$ is the plastic moment of the jth beam of the kth storey;
- $\overline{m}_{r,jk}$ is the nondimensional plastic moment of the right end beam-to-column joint of the jth bay of the kth storey;
- $\overline{m}_{l,jk}$ is the nondimensional plastic moment of the left end beam-to-column joint of the jth bay of the kth storey;
- q_{jk} is the uniform vertical load acting on the jth beam of the kth storey;
- x_{jk} is the abscissa of the second plastic hinge of the jth beam of the kth storey, given by:

$$x_{jk} = L_j - \left(\frac{2 M_{b,jk} (\overline{m}_{r,jk} + 1)}{q_{jk}} \right)^{1/2} \tag{7}$$

$$\text{for} \quad q_{jk} > \frac{2 M_{b,jk}}{L_j^2} \left\{ (2 + \overline{m}_{r,jk} - \overline{m}_{l,jk}) + 2 [(\overline{m}_{r,jk} + 1) (1 - \overline{m}_{l,jk})]^{1/2} \right\}$$

while $x_{jk} = 0$ in the opposite case;

- $R_{b,jk}$ is a coefficient related to the participation of the jth beam of the kth storey to the collapse mechanism; in addition, this coefficient accounts for the magnitude of the rotations of the plastic hinges resulting:

$$R_{b,jk} = \frac{L_j}{L_j - x_{jk}} \tag{8}$$

when the jth beam of the kth storey participate to the collapse mechanism and $R_{b,jk} = 0$ in the opposite case;

- $R_{c,ik}$ is a coefficient accounting for the participation of the ith column of the kth storey to the collapse mechanism, being:
  $R_{c,ik} = 2$ when the column is yielded at both ends
  $R_{c,ik} = 1$ when only one column end is yielded
  $R_{c,ik} = 0$ when the column does not participate to the collapse mechanism;
- $D_{v,jk}$ is a coefficient, related to the external work of the uniform load acting on the jth beam of the kth storey, given by:

$$D_{v,jk} = \frac{L_j x_{jk}}{2} \tag{9}$$

when the jth beam of the kth storey participate to the collapse mechanism and $D_{v,jk} = 0$ in the opposite case;

- $F^T = | F_1 , F_2 , \ldots\ldots\ldots , F_k , \ldots\ldots\ldots , F_{n_s} |$ is the vector of the design horizontal forces, where F_k is the horizontal force applied to the kth storey;
- $h^T = | h_1 , h_2 , \ldots\ldots\ldots , h_k , \ldots\ldots\ldots , h_{n_s} |$ is the vector of the storey heights, where h_k is the height of the kth storey;
- s is the shape vector of the storey horizontal virtual displacements ($du = s\, d\theta$, where $d\theta$ is the virtual rotation of the plastic hinges of the columns involved in the mechanism;

- $V^T = \{ V_1 , V_2 , ... , V_k , ... , V_{n_s} \}$ is the vector of the storey vertical loads, where V_k is the total vertical load acting at the kth storey given by:

$$V_k = \sum_{j=1}^{n_b} q_{jk} L_j \tag{10}$$

- $\boldsymbol{B}$ is a matrix of order $n_b \times n_s$ accounting for the location of the plastic hinges within the beams, the element B_{jk} of $\boldsymbol{B}$ is defined as:

$$B_{jk} = \frac{\overline{m}_{l,jk} + \overline{m}_{r,jk}}{2} M_{b,jk} \quad \text{for} \quad x_{jk} = 0 \tag{11}$$

and:

$$B_{jk} = \frac{1 + \overline{m}_{r,jk}}{2} M_{b,jk} \quad \text{for} \quad x_{jk} > 0 \tag{12}$$

- $\boldsymbol{C}$ is the matrix of order $n_c \times n_s$ whose elements C_{ik} are equal to the column plastic moments (i.e. $C_{ik} = M_{c,ik}$);
- $\boldsymbol{R}_b$ is the matrix (order $n_b \times n_s$) of the coefficients $R_{b,jk}$;
- $\boldsymbol{R}_c$ is the matrix (order $n_c \times n_s$) of the coefficients $R_{c,ik}$;
- $\boldsymbol{D}_v$ is the matrix (order $n_b \times n_s$) of the coefficients $D_{v,jk}$;
- $M_k^T = \{ M_{c,1k} , M_{c,2k} , ... , M_{c,ik} , ... , M_{c,n_c k} \}$ is the vector of the plastic moments of the columns of the kth storey, reduced due to the influence of the axial force;
- $\boldsymbol{q}$ is the matrix (order $n_b \times n_s$) of the uniform loads acting on the beams.

3.2 Mechanism equilibrium curves

As already pointed out, the collapse mechanisms of moment resisting frames under seismic horizontal forces can be considered belonging to three main typologies (Fig.1). The collapse mechanism of the global type is a particular case of type 2 mechanism.
The linearized mechanism equilibrium curve can be always expressed as:

$$\alpha_c = \alpha - \gamma \delta \tag{13}$$

where α is the kinematically admissible multiplier of horizontal forces and γ is the slope of the mechanism equilibrium curve.

Concerning the evaluation of the kinematically admissible multiplier of horizontal forces corresponding to the generic mechanism, it is easy to recognize that, for a virtual rotation $d\theta$ of the plastic hinges of the columns involved in the mechanism, the internal work can be expressed as:

$$W_i = [tr(\boldsymbol{C}^T \boldsymbol{R}_c) + 2\, tr(\boldsymbol{B}^T \boldsymbol{R}_b)]\, d\theta \tag{14}$$

where tr denotes the trace of the matrix.

The external work due to the horizontal forces and to the uniform load acting on the beams can be written as:

$$W_e = [\alpha \boldsymbol{F}^T \boldsymbol{s} + tr(\boldsymbol{q}^T \boldsymbol{D}_v)]\, d\theta \tag{15}$$

Therefore the application of the virtual work principle provides the kinematically admissible multiplier as:

$$\alpha = \frac{[tr(\boldsymbol{C}^T \boldsymbol{R}_c) + 2\, tr(\boldsymbol{B}^T \boldsymbol{R}_b) - tr(\boldsymbol{q}^T \boldsymbol{D}_v)]}{\boldsymbol{F}^T \boldsymbol{s}} \tag{16}$$

In order to compute the slope of the mechanism equilibrium curve, it is necessary to evaluate the second order work due to vertical loads. With reference to Fig.4, it can be observed that the horizontal displacement of the kth storey involved in the generic mechanism is given by $u_k = r_k \sin\theta$, where r_k is the distance of the kth storey from the center of rotation C and θ the angle of rotation.

The top sway displacement is given by $\delta = H_a \sin\theta$, where H_a is the sum of the interstorey heights of the storeys involved by the generic mechanism.

The relationship between vertical and horizontal virtual displacements is given by $dv_k = du_k \sin\theta$. It shows that, as the ratio dv_k/du_k is independent of the considered storey, vertical and horizontal virtual displacement vectors have the same shape. In fact, the virtual horizontal displacements are given by $du_k = r_k\, d\theta$, where r_k defines the shape of the virtual horizontal displacement vector, while the virtual vertical displacements are given by $dv_k = (\delta / H_o)\, r_k\, d\theta$ and, therefore, they have the same shape r_k of the horizontal ones. It can be concluded that:

$$dv = \frac{\delta}{H_o}\, s\, d\theta \tag{17}$$

As a consequence, the second order work due to vertical loads is given by:

$$W_v = V^T s \frac{\delta}{H_o}\, d\theta \tag{18}$$

Therefore, the slope of the mechanism equilibrium curve is given by:

$$\gamma = \frac{V^T s \frac{1}{H_o}}{F^T s} \tag{19}$$

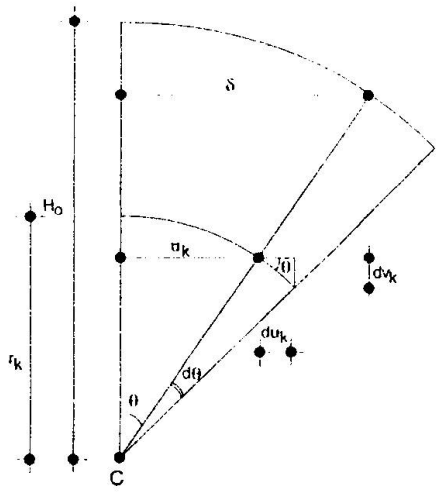

Fig.4 - Vertical displacements

The following notation will be used to denote the parameters of the equilibrium curve of the considered mechanisms:

- $\alpha^{(g)}$ and $\gamma^{(g)}$ are, respectively, the kinematically admissible multiplier of the horizontal forces (rigid-plastic theory) and the slope of the softening branch of the α–δ curve, corresponding to the global type mechanism;
- $\alpha_{i_m}^{(t)}$ and $\gamma_{i_m}^{(t)}$ have the same meaning of the previous symbols, but they are referred to the i_mth mechanism of the tth typology (t=1,2,3).

The expressions of the above parameters will be furtherly developed in order to evidence the contribution of the columns to the internal work.

3.3 Global type mechanism

In the case of global type mechanism (Fig.1), the shape vector of the horizontal displacements is given by $s^{(g)} = h$. In addition, as all storeys participate to the collapse mechanism, all beams are involved. This is taken into account through the matrix $R_b^{(g)}$ related to the rotation of the plastic hinges and the matrix $D_v^{(g)}$ related to the beam vertical displacements. $R_b^{(g)}$ is the value of R_b and $D_v^{(g)}$ is the value of D_v for the specific case of global mechanism.

Therefore, the kinematically admissible multiplier is given by:

$$\alpha^{(g)} = \frac{M_{c1}^l\, I + 2\, tr(B^T R_b^{(g)}) - tr(q^T D_v^{(g)})}{F^T s^{(g)}} \tag{20}$$

where I is the unit vector of order n_c. In addition, taking into account that $H_o = h_{n_s}$, because all storeys are involved in the collapse mechanism, the slope $\gamma^{(g)}$ of the mechanism equilibrium curve is obtained from equation (19) for $s = s^{(g)}$ and $H_o = h_{n_s}$.

3.4 Type-1 mechanisms

With reference to the i_mth mechanism of type-1 (Fig.1), the shape vector of the horizontal displacements can be written as:

$$s_{i_m}^{(1)\,T} = \left| h_1 , h_2 , h_3 , \ldots\ldots , h_{i_m} , h_{i_m} , h_{i_m} \right| \tag{21}$$

where the first element equal to h_{i_m} corresponds to the i_mth component.
The kinematically admissible multiplier corresponding to the i_mth mechanism of type-1 is given by:

$$\alpha_{i_m}^{(1)} = \frac{\boldsymbol{M}_{ci_m}^T \boldsymbol{I} + 2\, tr(\boldsymbol{B}^T \boldsymbol{R}_{b_{i_m}}^{(1)}) + \boldsymbol{M}_{ci_m}^T \boldsymbol{I} - tr(\boldsymbol{q}^T \boldsymbol{D}_{v_{i_m}}^{(1)})}{\boldsymbol{F}^T \boldsymbol{s}_{i_m}^{(1)}} \tag{22}$$

where $\boldsymbol{R}_{b_{i_m}}^{(1)}$ is the value of $\boldsymbol{R}_b$ for the i_mth mechanism of this type and $\boldsymbol{D}_{v_{i_m}}^{(1)}$ is the value of $\boldsymbol{D}_v$ for the i_mth mechanism of type-1.
In addition, only the first i_m storeys participate to the collapse mechanism, so that $H_o = h_{i_m}$. As a consequence, the slope $\gamma_{i_m}^{(1)}$ of the mechanism equilibrium curve is still computed through equation (19), but assuming $s = s_{i_m}^{(1)}$ and $H_o = h_{i_m}$.

3.5 Type-2 mechanisms

With reference to the i_mth mechanism of type-2 (Fig.1), the shape vector of the horizontal displacements can be written as:

$$\boldsymbol{s}_{i_m}^{(2)\,T} = \{\, 0\,,\, 0\,,\, 0\,,\, ...\,,\, 0\,,\, h_{i_m} - h_{i_m-1}\,,\, h_{i_m+1} - h_{i_m-1}\,,\, ...\,,\, h_n - h_{i_m-1} \,\} \tag{23}$$

where the first non-zero element is the ith one.
The kinematically admissible multiplier corresponding to the i_mth mechanism of the type-2 is given by:

$$\alpha_{i_m}^{(2)} = \frac{\boldsymbol{M}_{ci_m}^T \boldsymbol{I} + 2\, tr(\boldsymbol{B}^T \boldsymbol{R}_{b_{i_m}}^{(2)}) - tr(\boldsymbol{q}^T \boldsymbol{D}_{v_{i_m}}^{(2)})}{\boldsymbol{F}^T \boldsymbol{s}_{i_m}^{(2)}} \tag{24}$$

where $\boldsymbol{R}_{b_{i_m}}^{(2)}$ is the value of $\boldsymbol{R}_b$ for the i_mth mechanism of type-2 and $\boldsymbol{D}_{v_{i_m}}^{(2)}$ is the corresponding value of the matrix $\boldsymbol{D}_v$.
In addition, the i_mth storey and those above it participate to the mechanism. Therefore, the slope of the mechanism equilibrium curve is obtained from equation (19) with $H_o = h_n - h_{i_m-1}$ and $s = s_{i_m}^{(2)}$.

3.6 Type-3 mechanisms

Finally, with reference to the i_mth mechanism of type-3 (Fig.1), the shape vector of the horizontal displacements can be written as:

$$\boldsymbol{s}_{i_m}^{(3)\,T} = \{\, 0,\, 0,\, ..\, 0,\, 1,\, 1,\, 1,\, ...,\, 1 \,\}\ (h_{i_m} - h_{i_m-1}) \tag{25}$$

where the first term different from zero is the i_mth one.
Moreover, both the matrix $\boldsymbol{R}_{b_{i_m}}^{(3)}$ and the matrix $\boldsymbol{D}_{v_{i_m}}^{(3)}$ are null matrix, because in this mechanism there is not any beam participating to the collapse mechanism. Therefore, the kinematically admissible multiplier of the i_mth mechanism of type-3 is given by:

$$\alpha_{i_m}^{(3)} = \frac{2\, \boldsymbol{M}_{ci_m}^T \boldsymbol{I}}{\boldsymbol{F}^T \boldsymbol{s}_{i_m}^{(3)}} \tag{26}$$

which accounts for the fact that the columns of the i_mth storey are yielded at both ends.
As the i_mth storey only is involved in the mechanism $H_o = h_{i_m} - h_{i_m-1}$, and the corresponding slope $\gamma_{i_m}^{(3)}$ of the mechanism equilibrium curve can be obtained by substituting this value in equation (19) where also $s = s_{i_m}^{(3)}$ has to be assumed.

4. Failure mode control

4.1 Design conditions

In order to design frames failing in global mode, the cross-sections of columns have to be dimensioned so that, according to the upper bound theorem, the kinematically admissible

horizontal force multiplier corresponding to the global type mechanism is the minimum among all kinematically admissible multipliers.

This condition is sufficient to assure the desired collapse mechanism provided that the structural material behaves as rigid-plastic so that the horizontal displacements are equal to zero up to the complete development of the collapse mechanism. On the contrary, the actual behaviour is elasto-plastic with significant displacements before the complete development of the collapse mechanism. These displacements give rise to second order effects which cannot be neglected in the design process, particularly in the case of semirigid frames.

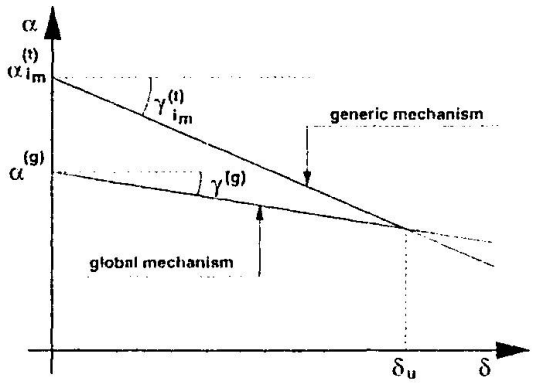

Fig.5 - Design requirements

From the practical point of view, the influence of second order effects can be taken into account by imposing that the mechanism equilibrium curve corresponding to the global mechanism has to lie below those corresponding to all other mechanisms. However, the fulfilment of this requirement is necessary only up to a selected ultimate displacement δ_u which has to be compatible with the plastic rotation capacity of members and/or connections ($\delta_u = \theta_{p_u} h_{n_s}$) (Fig.5).

Therefore, the following design conditions have to be imposed:

$$\alpha^{(g)} - \gamma^{(g)}\,\delta_u \le \alpha^{(t)}_{i_m} - \gamma^{(t)}_{i_m}\,\delta_u \qquad i_m = 1,2,3,.....,n_s \qquad t = 1,2,3 \tag{27}$$

This means that there are $3n_s$ design conditions to be satisfied in the case of a frame having n_s storeys. These conditions, which derive directly from the extension of the upper bound theorem to the mechanism equilibrium curves, will be integrated by conditions related to technological limitations.

4.2 Conditions to avoid undesired mechanisms

As an example, the method for deriving the design conditions to be satisfied to avoid any undesired collapse mechanism will be presented with reference to type-1 mechanisms only. The extension to the other collapse mechanism typologies can be developed in analogous way. Even though considering full-strength connections only, the complete series of design conditions (i.e. including those for type-2 and type-3 mechanisms) are given in references [2,3].

The n_s conditions given by relationship (27) for $t=1$ can be conveniently expressed by introducing the following parameters:

$$\mu^{(g)} = 2\,tr\,(\boldsymbol{B}^T \boldsymbol{R}_b^{(g)}) \qquad \nu^{(g)} = \frac{1}{h_{n_s}} \boldsymbol{V}^T \boldsymbol{s}^{(g)} \qquad \tau^{(g)} = tr\,(\boldsymbol{q}^T \boldsymbol{D}_v^{(g)}) \tag{28}$$

With reference to the global mechanism, the parameter $\mu^{(g)}$ represents the internal work developed by the beams and/or the connections, the parameter $\tau^{(g)}$ is the external work due to the uniform loads acting on the beams, while the parameter $\nu^{(g)}$ is related to the second order work due to vertical loads. These parameters are known quantities, because it is intended that a preliminary design of beams and connections has been carried out according to the procedure suggested in [5,6] while the values of vertical loads are data of the design problem.

In addition, it is useful to introduce the following non-dimensional functions of the mechanism index i_m:

$$\xi_{i_m} = \frac{2\,tr\,(\boldsymbol{B}^T \boldsymbol{R}_{b_{i_m}}^{(t)})}{2\,tr\,(\boldsymbol{B}^T \boldsymbol{R}_b^{(g)})} = \frac{2\,tr\,(\boldsymbol{B}^T \boldsymbol{R}_{b_{i_m}}^{(t)})}{\mu^{(g)}} \qquad \lambda_{i_m} = \frac{\boldsymbol{F}^T \boldsymbol{s}_{i_m}^{(t)}}{\boldsymbol{F}^T \boldsymbol{s}^{(g)}} \tag{29}$$

$$\zeta_{i_m}^{(1)} = \frac{tr(q^T D_{v_{i_m}}^{(1)})}{tr(q^T D_v^{(g)})} = \frac{tr(q^T D_{v_{i_m}}^{(1)})}{\tau^{(g)}} \tag{30}$$

The function ξ_{i_m} represents the ratio between the internal work which the beams and/or the connections develop in the i_mth mechanism of type-1 and that developed in the global mechanism. The function λ_{i_m} represents the ratio between the external work which the horizontal forces develop in the i_mth mechanism of type-1 and that developed in the global mechanism. Finally, the function ζ_{i_m} represents tha ratio between the external work which the uniform vertical loads develop in the i_mth mechanism of type-1 and that developed in the global mechanism. All these functions are known, because the plastic moments of beams ($M_{b,jk}$) and of connections ($\overline{m}_{l,jk}$ and $\overline{m}_{r,jk}$) are known. In fact, the beam sections are designed to resist vertical loads. In addition, both the horizontal forces F_k and the uniform loads q_{jk} are assigned.

Moreover, in order to account for the influence of second order effects, an additional function related to the slopes of the mechanism equilibrium curves has to be defined:

$$\Delta_{i_m}^{(1)} = \frac{F^T s^{(g)}}{F^T s_{i_m}^{(1)}} \frac{\frac{1}{h_{i_m}} V^T s_{i_m}^{(1)}}{\frac{1}{h_{n_s}} V^T s^{(g)}} = \frac{1}{\lambda_{i_m}} \frac{\frac{1}{h_{i_m}} V^T s_{i_m}^{(1)}}{v^{(g)}} \tag{31}$$

The parameter $\Delta_{i_m}^{(1)}$ represents the ratio between the slope of the equilibrium curve of the i_mth mechanism of type-1 and that of the global mechanism.

In addition, it is convenient to introduce the following parameter:

$$\rho_{i_m}^{(1)} = \frac{M_{c,i_m}^T I}{M_{c1}^T I} = \frac{\sum_{i=1}^{n_c} M_{c,ii_m}}{\sum_{i=1}^{n_c} M_{c,i1}} \tag{32}$$

which is the ratio between the sum of the reduced plastic moments of the i_mth storey columns and the same sum corresponding to the first storey columns.

By means of the above parameters, the i_mth condition to be satisfied to avoid type-1 collapse mechanisms can be written in the following form:

$$\rho_{i_m}^{(1)} \geq \frac{\left(1 - \frac{1}{\lambda_{i_m}}\right) \sum_{i=1}^{n_c} M_{c,i1} + \left(1 - \frac{\xi_{i_m}}{\lambda_{i_m}}\right) \mu^{(g)} + v^{(g)} \left(\Delta_{i_m}^{(1)} - 1\right) \delta + \tau^{(g)} \left(\frac{\zeta_{i_m}^{(1)}}{\lambda_{i_m}} - 1\right)}{\frac{1}{\lambda_{i_m}} \sum_{i=1}^{n_c} M_{c,i1}} \tag{33}$$

which has to be applied for $i_m = 1,2,3,.....n_s$.

The design conditions to be satisfied to avoid type-2 and type-3 collapse mechanisms are obtained in similar way, leading to other two series of parameters ($\rho_{i_m}^{(2)}$ and $\rho_{i_m}^{(3)}$). These parameters are still defined as the ratio between the sum of the reduced plastic moments of the columns of the i_mth storey and the same sum corresponding to the first storey, but they provide the values of this ratio to avoid type-2 and type-3 mechanisms [2,3].

Obviously, as these design conditions have to be contemporaneously satisfied for each storey, the ratios ρ_{i_m} ($\rho_{i_m} = M_{ci_m} I / M_{c1} I$) has to satisfy the following relationship:

$$\rho_{i_m} = \max \left\{ \rho_{i_m}^{(1)}, \rho_{i_m}^{(2)}, \rho_{i_m}^{(3)} \right\} \tag{34}$$

In addition, as the section of columns can only decrease along the height of the frame, the values of ρ_{i_m} (with $i_m = 1,2,....,n_s$) obtained by means of the conditions derived through the

application of the upper bound theorem have to be modified in order to satisfy the following technological limitation:

$$\rho_1 \geq \rho_2 \geq \rho_3 \geq \ldots\ldots\ldots \geq \rho_{n_s} \tag{35}$$

4.3 Evaluation of the axial load in the columns at the collapse state

If the sum of the reduced plastic moments of columns of the first storey is specified, then the previously explained design conditions allow the definition, through the ratios ρ_k ($k=1,2,\ldots,n_s$), of the same sum corresponding to the kth storey, which guarantees that failure does not occur according to mechanisms belonging to the three examined typologies. In order to define the plastic section modulus of the columns, the evaluation of the axial load in the columns at the collapse state is required.

The evaluation of the column axial forces can be performed taking into account that, at the collapse state, the shear forces transmitted by the beams are given by:

$$S = \frac{qL}{2} \pm \frac{2(\overline{m}_r + \overline{m}_l) M_b}{L} \tag{36}$$

provided that the limit value of the uniform vertical load is not exceeded (i.e. equation (5) is not satisfied) and by:

$$S = \frac{qL}{2} \pm \frac{M_{ri} + \overline{m}_r M_b}{L} \tag{37}$$

where M_{ri} is provided by equation (4), in the opposite case.

Both in equation (36) and in equation (37), for positive horizontal forces (from left towards right), the sign plus is referred to the right end of the beam and the sign minus is referred to the left end of the beam.

The sum of these shear forces transmitted by the beams at each storey, above the considered one, provides the axial forces in the columns of the considered storey.

4.4 Design algorithm

It has been pointed out that the upper bound theorem allows the assessment of a condition for avoiding each undesired collapse mechanism. As three different collapse mechanism typologies have been considered, there are $3n_s$ design conditions to be satisfied. These design conditions have to be integrated by the technological condition (35). The above mentioned relationships can be used to design frames failing in global mode and, therefore, having a mechanism equilibrium curve given by equation (13), with the kinematically admissible multiplier of horizontal forces given by equation (20) and the slope given by relationship (19) (with $H_{ri} = h_{ri}$ and $s = s^{(g)}$). The fulfilment of the above design requirements is a linear programming problem which can be solved through the algorithm already described in [2,3].

5. Design procedure

The main difficulty in the elastic design of semirigid frames is due the fact that the internal actions, which the members and the joints have to withstand, depend on the joint rotational stiffness whose value, in turn, affects the flexural resistance that the joints are able to provide [5,6]. This difficulty can be overcome provided that a plastic design approach, such as that previously described, is adopted. Notwithstanding, some iterations can be required as soon as serviceability requirements are also considered. In fact, the fulfilment of a given limit concerning the interstorey drift or the top sway displacement can lead to the need to increase the joint rotational stiffness and/or the beam sizes. In such a case, the increase of the plastic internal work due to the beams (the joint flexural resistance increases as the joint rotational stiffness increases) can undermine the expected failure mode, so that the plastic design for failure mode control has to be repeated starting from the new beam-to-column joint details and/or the new beam sizes. As a consequence, the complete design procedure can be based on the following steps, where the plastic method of design for failure mode control, previously described, has to be intended as a «subroutine» only of the proposed design method:

a) perform a preliminary design of beams (i.e. $M_{b,jk}$), connections and columns to withstand vertical loads only. This step can be accomplished through the method described in [5,6]. According to Eurocode 3 [7], the combination of actions $1.35\ G_k + 1.5\ Q_k$ has to be considered for the ultimate limit state and the combination $G_k + Q_k$ for the serviceability limit state;
b) compute the preliminary values of the joint flexural resistance ($\overline{m}_{r,jk}$ and $\overline{m}_{l,jk}$) through the component method [8];
c) design the column sections to assure a collapse mechanism of global type (i.e. through the plastic design method described in the previous section), starting from the preliminary values of $M_{b,jk}$, $\overline{m}_{r,jk}$ and $\overline{m}_{l,jk}$. According to Eurocode 8 [9], the vertical loads to be considered in this step are those corresponding to the load combination $G_k + \psi_2\ Q_k$ while the seismic horizontal forces have to be computed accounting for the presence of all gravity loads appearing in the combination $G_k + \sum\ \psi_{E,i}\ Q_{ki}$;
d) modify, if necessary, the structural detail of beam-to-column joints to keep constant the $\overline{m}$ values. In fact, as the previous step leads generally to column sections greater than those obtained from preliminary design (step **a**), the joint flexural resistance could increase (this depends on the weakest joint component) undermining the expected collapse mechanism;
e) compute the joint rotational stiffness through the component method;
f) check the beams, the joints, the interstorey drifts and the top sway displacement for the loading condition $\sum G_{ki} + \gamma_I A_{Ed} + \sum \psi_{2i}\ Q_{ki}$ [9]. If anyone of the above checks is not satisfied, modify the beam sizes or the joint structural detail (increasing $\overline{m}$ and the joint rotational stiffness) and return to step **c**.

6. Conclusions

A new method to design semirigid frames failing in global mode has been presented in this paper. The method is based on the extension of the kinematic theorem of plastic collapse to the concept of mechanism equilibrium curve. This allows to include into the design process the influence of second order effects, which play a very important role in the seismic design of steel frames, particularly in the case of semirigid frames.

In addition, a complete design procedure including the fulfilment of the serviceability requirements has been proposed.

7. References

[1] **F.M. Mazzolani, V. Piluso**: Failure Mode and Ductility Control of Seismic Resistant MR-Frames, Costruzioni Metalliche, N.2, pp. 11-28, 1995.
[2] **F.M. Mazzolani, V. Piluso**: A new method to design steel frames failing in global mode including P-Δ effects, in Behaviour of Steel Structures in Seismic Areas edited by F.M. Mazzolani and V. Gioncu, Proceedings of the International Workshop (Timisoara, Romania, 26 June - 1 July, 1994), E & FN SPON, an Imprint of Chapman & Hall, pp. 300-309, 1995.
[3] **F.M. Mazzolani, V. Piluso**: Plastic Design of Seismic Resistant MR-Frames, submitted for publication to Earthquake Engineering and Structural Dynamics, January, 1996.
[4] **F.M. Mazzolani, V. Piluso**: Seismic design criteria for moment resisting steel frames, in Steel Structures edited by A.N. Kounadis, Proceedings of the 1st European Conference on Steel Structures (Athens, Greece, 18-20 May, 1995), Balkema, pp. 247-254, 1995.
[5] **C. Faella, V. Piluso, G. Rizzano**: Design of Braced Frames with Extended End Plate Connections, submitted for pubblication to Journal of Constructional Steel Research, December, 1995.
[6] **C. Faella, V. Piluso, G. Rizzano**: A New Design Approach for Braced Frames with Extended End Plate Connections, IABSE International Colloquium on Semirigid Structural Connections, Istanbul, 25-27 September, 1996.
[7] **Commission of the European Communities**: Eurocode 3: design of steel structures, 1990
[8] **Eurocode 3, part 1.1**: Revised Annex J: Joints in Building Frames
[9] **Commission of the European Communities**: Eurocode 8: European Code for Seismic Regions, ENV, November 1994.

Leere Seite
Blank page
Page vide

DESIGN HANBOOK FOR FRAME DESIGN

INCLUDING JOINT BEHAVIOUR

Jean-Pierre JASPART
Research Associate FNRS
Doctor Engineer
University of Liège
Liège
BELGIUM

Jean-Pierre Jaspart, born 1962, got his Civil Engineering Degree in 1985 and his Ph.D Thesis in 1991. He is the author of more than 60 papers on connection and frame design, member of the Drafting Group of Annex J of Eurocode 3 and Chairman of the COST C1 Working Group on "Steel and Composite Connections".

René MAQUOI
Professor
Doctor Engineer
University of Lège
Liège
BELGIUM

René Maquoi, born 1942, got his Civil Engineering Degree in 1965 and his Ph.D Thesis in 1973. He is the author or coauthor of more than 200 papers mostly devoted to stability problems and design of connections. He is involved in various international activities: preparation of Eurocode 3, chairmanship or membership of ECCS and SSRC, task working groups, ...

Summary

In this paper, a design handbook for designers of steel building frames is presented. This handbook gives a quite complete overview of the design procedures for frame design - including joint behaviour - which are included in Eurocode 3 Part 1-1[1]. In its first part, a background information is given. The second part focuses on application rules for daily practice and a particular attention is paid to structural joints. Finally, worked examples for complete frame design are presented in the third part.

1. Introduction

Traditionally the analysis and the design of steel frame structures is based on the assumption that the constitutive beam-to-column joints, splices and column bases are perfectly pinned or perfectly rigid.

However studies performed in the last decade have clearly shown that:

- Most of the joints used in daily practice are not fulfulling the requirements so to be characterized by such idealized responses; they are said *«semi-rigid»* and «partial strength» when their resistance is lower than that of the connected members.
- The fulfillment of these requirements is often involving extra fabrication or erection costs .

Through economical investigations, it has also been progressively demonstrated that:

- The traditional rules for design of joints are rather conservative.
- The use of semi-rigid joints instead of pinned ones results in a decrease of the weight of the structure, and therefore of their total cost (5 to 10 %) including fabrication, transportation and erection costs.
- The use of semi-rigid joints instead of rigid ones sometimes results in an increase of the amount of steel needed, but also to a strong decrease of the fabrication costs through a simplified detailling of the joints (less stiffening for instance). The benefits varies here from 10 to 25 %.

To profit from these potential benefits requires new design methodologies for what regards design assumptions,frame analysis and verification of the ultimate and serviceability limit states.

This need is now widely expressed by designers, what has engendered, at the european level, different actions in the last years . Among these ones, let us mention:

- The full revision of the Annex J of Eurocode 3 on "Steel Joints in Building Frames" [2].
- The SPRINT european project where simplified design procedures for joint design and tables of standardized joints, all in agreement with EC3 Annex J, have been suggested [3].

The first one provides a legal frame for the use of the new design techniques for joints while the second focuses more on the practical aspects to which the designer is likely to be faced in his daily practice.

In the frame of a recent ECSC project (contracts 7210-SA/212 and 320), the SPRINT action has been prolonged so to cover also the implications of the joint behaviour on the structural frame analysis and design. The guide for users resulting from this action is briefly presented in the following pages.

The partners in this project are: University of Liège in Belgium as coordinator (R. MAQUOI and J.P. JASPART), CTICM in France (B. CHABROLIN, I. RYAN and A. SOUA), CRIF in Belgium (D. VANDEGANS), TNO Delft in The Netherlands (M. STEENHUIS) and RWTH Aachen in Germany (K. WEYNAND).

2. Content of the design handbook

The ECSC user's manual covers the following three main aspects :

- The design of commonly used beam-to-column joint configurations such as welded ones or bolted end plate and flange cleated ones. Beam splices are also covered.
- Guidelines on how to incorporate joint behaviour in the structural analysis (both 1st order and 2nd order, elastic and plastic).
- Design checks for the ultimate limit states (frame and member resistance and stability, member and joint section checks, ...)

It is structured into three main parts which all deal with all the three different aspects mentioned here above:

- *Part 1-Technical Background*

  A primary objective of the manual is to facilitate the use of Eurocode 3 and it has so been thought that this was requiring explanations about the general design philososophy to adopt in particular cases, the successive steps to follow, the assumptions to follow and the formulae to use.

- *Part 2-Application Rules*

  In this section, practical guidelines are given in a straigthforward manner. The designer should find there the recommendations he needs to perform frame analysis, joint design and structural verifications. All the formulae are expressed together with their limitations and their implications on further steps. For joints, three different design approaches are expressed, as described in section 3 of the present paper.

- *Part 3-Worked Examples.*

  Three different worked examples are included in the manual. They cover the whole frame and joint design procedure and not only some specific aspects as the joint characterization or the frame analysis. They should help the designer in understanding the different steps of a semi-rigid frame design, and the sequence of these steps according to the practical situation to which he is faced : engineer or constructor responsible for both frame and joint design or share of the responsibilities between the engineer (frame design) and the constructor (joint design).

All the scientific aspects have been disregarded and the content of all the chapters has been limited to the minimum but sufficient information which appears to be strictly useful to practitioners.

3. Design of the structural joints

An important step in the design process is the determination of the mechanical properties of the joints in terms of rotational stiffness, moment and shear resistances and rotation capacity.

For what regards this characterization, three approaches are followed :

- *design sheets*

  These are short documents containing very simple rules allowing to calculate in an easy and quick way the stiffness and resistance properties of some well-defined types of joints:

- beam-to column joints with extended endplates;
- beam-to column joints with flush endplates (2 types);
- beam splices with flush endplates (2 types);
- beam-to column joints with angle flange cleats.

These simplified procedures strongly reduce the amount of calculation in comparaison with the application of EC3 Annex J but are anyway in agreement with the EC3 design philosophy. An example of such a design sheet is shown in Annex 1 of the present paper.

- *design tables*

These are tables covering standardized joints and providing the user with joint detailing and stiffness / resistance properties (see Annex 2); information allowing to classify the joints as pinned, semi-rigid or rigid, partial strength or full strength is also given.

- *software*

This PC software called DESIMAN is able to characterize the mechanical properties of a wide range of usual or non-usual types of joints subjected to bending moments and shear forces. It includes graphical pre- and post-processors (see Annex 3). The pre-processor allows a user's friendly introduction of the data. It is connected to bolt, plate, material and profile databases, so allowing a decrease of the time required to introduce the data. It is also connected to another database in which all the calculations made can be stored, in order to be used further if needed.
The post-processor of DESIMAN produces four main files :

- A short one just giving the main results of the computation : design resistances in bending and shear, initial stiffness, collapse mode, ductility, class for frame analysis (1/2 page).
- The previous one to which the resistance and the stiffness of all the constitutive joint components are added. Such a file allows the designer to modify in an optimum way its joint when the design requirements are not fulfilled (1 page).
- A calculation note (± 5 pages) presenting more detailed results of the calculations, for each component and for the joint. This note is useful when, for instance, the design has to be checked by a control office.
- A full calculation note just like that which could be produced by hand, and in which the results of all the intermediate calculations are given.

4. References

[1] Eurocode 3: Design of Steel Structures, Part 1-1; General Rules and Rules for Buildings, ENV 1993-1-1, 1992.

[2] New revised Annex J of Eurocode 3 "Joints in Building Frames", Doc. CEN/TC250/SC3-N419E, Brussels, June 1994.

[3] SPRINT Contract RA351 on "Steel Moment Connections according to Eurocode 3. Simple Design Aids for Rigid and Semi-Rigid Joints", 1992-1996.

Annex 1: Example of simplified design procedure

Mechanical characteristics

	Yield stresses	Ultimate stresses
Beam webs	f_{ywb}	-
Beam flanges	f_{yfb}	-
End-plates	f_{yp}	f_{up}
Bolts	-	f_{ub}

If hot-rolled profiles : $f_{ywb} = f_{yfb}$

Geometrical characteristics

Joint

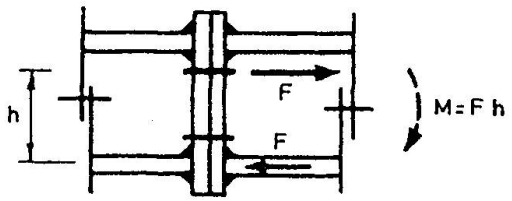

Beams

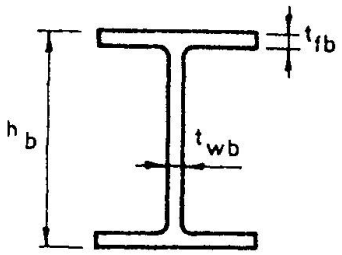

End-plates

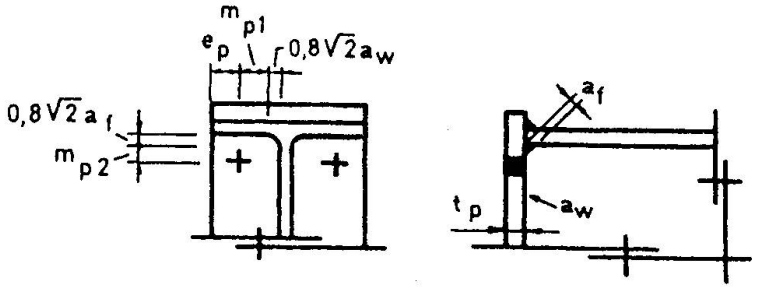

Bolts

d_w : see figure or = d_p if no washer*

A_s : resistance area of the bolt

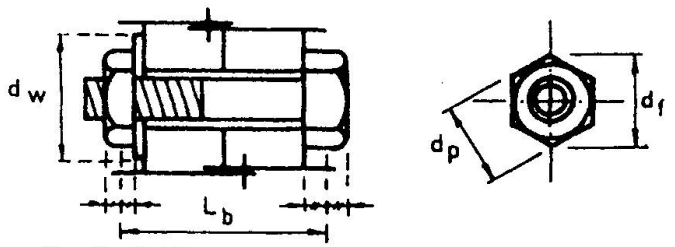

* d_r is recommended in EC3 Annex J, and not d_p. As d_r is not given in all the catalogs for bolts, d_p is chosen here (safe assumption).

	STIFFNESS	*RESISTANCE*
Beam flanges in compression	$k_3 = \infty$	$F_{Rd,3} = M_{c,Rd} / (h_b - t_{fb})$ $M_{c,Rd}$: beam design moment resistance
Bolts in tension	$k_4 = 1{,}6 \dfrac{A_s}{L_b}$	$F_{Rd,4} = 2\ B_{t,Rd}$ *with* $B_{t,Rd} = F_{t,Rd}$ $F_{t,Rd} = \dfrac{0{,}9\ f_{ub}\ A_s}{\gamma_{Mb}}$
End-plates in bending	$k_7 = \dfrac{0{,}85\ l_{eff,p,1}\ t_p^3}{2\ m_{p1}^3}$	$F_{Rd,7} = \min [\ F_{ep,Rd,1}\ ;\ F_{ep,Rd,2}\ ]$ $F_{ep,Rd,1} = \dfrac{(8n_p - 2e_w)\ l_{eff,p,1}\ m_{pl,p}}{2m_{p1}\ n_p - e_w(m_{p1} + n_p)}$ $F_{ep,Rd,2} = \dfrac{2\ l_{eff,p,1}\ m_{pl,p} + 2\ B_{t,Rd}\ n_p}{m_{p1} + n_p}$ $n_p = \min [\ e_p\ ;\ 1{,}25m_{p1}\ ]$ $m_{pl,p} = 0{,}25\ t_p^2\ f_{yp} / \gamma_{Mo}$ $e_w = d_w / 4$
	$l_{eff,p,1} = \min [\ 2\pi m_{p1}\ ;\ \alpha m_{p1}\ ]$ where α is defined in EC3 Annex J	
Beam web in tension	$k_8 = \infty$	$F_{Rd,8} = b_{eff,wb,1}\ t_{wb}\ f_{ywb} / \gamma_{Mo}$
	$b_{eff,wb,1} = l_{eff,p,1}$	
JOINT	Initial stiffness : $S_{j,ini} = E\ h^2 / \sum_{i=3,4,7,8} 1/k_i$ Nominal stiffness : $S_j = S_{j,ini} / 3$	$F_{Rd} = \min [\ F_{Rd,j}\ ]$ Plastic design moment resistance : $M_{Rd} = F_{Rd}\ h$ Elastic moment resistance : $\frac{2}{3} M_{Rd}$

Annex 2: Example of design table for standardized joints

Mode de rupture	Code
Semelle de la poutre en compression	BFC
Boulons en traction	BT
Plat d'about soumis à flexion	EPT
Ame de la poutre en traction	BWT

$\gamma_{M0} = 1.10$

$\gamma_{Mb} = 1.25$

Poutre	Boulons hr8.8	Plat d'about: S235 (mm)			Détail du noeud (mm)						Soudures (mm)		Rigidité du noeud (kNm/rad)		Résistance			Mode de rupture	Longueur de référence(m)	
															Moment (kNm)		Cisaillement (kN)			
S235		t_p	b_p	h_p	p	p_p	e_{pl}	w	w_l	u	a_w	a_f	$S_{j,ini}$	$S_{j,ini}/3$	M_{Rd}	$2/3M_{Rd}$	V_{Rd}	Code	L_{bb}	L_{bu}
IPE220	M16	15	140	240	60	120	60	90	25	10	3	5	15433	5144	24.1	16.1	157	EPT	3.0-R	S
IPE240	M16	15	140	260	60	140	60	90	25	10	4	5	20098	6699	27.2	18.1	157	EPT	3.3-R	S
IPE270	M16	15	154	290	65	160	65	90	32	10	4	6	26826	8942	32.4	21.6	157	EPT	3.6-R	S
	M20	20	154	290	65	160	65	90	32	10	4	6	42892	14297	53.8	35.9	245	EPT	R	7.1-R
IPE300	M16	15	170	320	65	190	65	90	40	10	4	6	36564	12188	38.9	25.9	157	EPT	3.8-R	12.0-R
	M20	20	170	320	65	190	65	90	40	10	4	6	57607	19202	64.3	42.8	245	EPT	R	7.6-R
IPE330	M16	15	180	350	65	220	65	90	45	10	4	6	47398	15799	44.8	29.9	157	EPT	4.2-R	13.0-R
	M20	20	180	350	65	220	65	90	45	10	4	6	74007	24669	73.8	49.2	245	EPT	2.7-R	8.3-R
	M24	20	180	350	75	200	75	110	35	10	4	6	62600	20867	78.5	52.3	352	EPT	3.2-R	9.9-R
IPE360	M16	15	210	400	75	250	75	90	60	20	5	7	60854	20285	50.1	33.4	157	EPT	4.5-R	14.0-R
	M20	20	210	400	75	250	75	90	60	20	5	7	93626	31209	82.5	55.0	245	EPT	2.9-R	9.1-R
	M24	20	210	400	85	230	85	110	50	20	5	7	85645	28548	98.8	64.5	352	EPT	3.2-R	10.0-R
IPE400	M16	15	220	440	75	290	75	90	65	20	5	7	78661	26220	56.7	37.8	157	EPT	4.9-R	15.4-R
	M20	20	220	440	75	290	75	90	65	20	5	7	120698	40233	93.4	62.3	245	EPT	3.2-R	10.1-R
	M24	20	220	440	85	270	85	110	55	20	5	7	113428	37809	112.7	75.1	352	EPT	3.4-R	10.7-R
	M27	25	220	440	95	250	95	130	45	20	5	7	118284	39428	139.3	92.9	458	EPT	3.3-R	10.3-R
IPE450	M16	15	230	490	75	340	75	90	70	20	5	8	104399	34800	65.0	43.3	157	EPT	5.4-R	17.0-R
	M20	20	230	490	75	340	75	90	70	20	5	8	159614	53205	107.1	71.4	245	EPT	3.6-R	11.1-R
	M24	20	230	490	85	320	85	110	60	20	5	8	152172	50724	130.4	86.9	352	EPT	3.7-R	11.6-R
	M27	25	230	490	95	300	95	130	50	20	5	8	162176	54059	165.8	110.5	458	EPT	3.5-R	10.9-R
IPE500	M16	15	240	540	80	380	80	100	70	20	6	9	118633	39544	72.4	48.3	157	EPT	6.8-R	S

Annex 3: Input and output screens of DESIMAN software